Synthesis of azobenzene-peptides and their application as a photoresponsive inhibitor for ON/OFF photoswitching of the motility of kinesin-microtubule

（アゾベンゼン-ペプチドの合成とキネシン-微小管の運動機能の ON/OFF 光スイッチのための光応答性阻害剤としての応用）

A Thesis

Submitted for the Degree of

Doctor of Life Science

By

SUNIL KUMAR K R

Laboratory of Smart Molecules

Transdisciplinary Life Science Course

Graduate School of Life Science

Hokkaido University

Japan, 2014

TABLE OF CONTENTS

1. INTRODUCTION

Protein molecular motors are naturally evolved nanosized machines responsible for mechanical movement, which is essential for many biological functions, including cell division, movement, intracellular transport, and muscle contraction. Kinesin[1, 2] is one among such motor proteins[3] that converts chemical energy, derived from the hydrolysis of adenosine triphosphate (ATP), into mechanical work. The force generated in this process enables kinesin molecules with about 80 nm in size to actively transport designated nano cargo (e.g., vesicles, chromosomes, organelles) to predetermined sites along microtubules with about 25 nm in diameter and with an average length of 25 μm, which are cytoskeletal tracks within a cell.[4-6] The properties of motor proteins—nanometer scale, high fuel efficiency, and force-generating capabilities—make them attractive alternatives to man-made motors, resulting in their use as key components for the construction of highly efficient nanotransport systems.[7–12] One vision is that the systems based on motor proteins will be used for controlled cargo manipulation on chips, with applications in sorting, separation, purification, or assembly of materials.[13, 14] In the last decade, microtubules have been employed extensively as shuttles to transport attached cargo (e.g., polystyrene beads,[15] quantum dots[16] and DNA molecules[17, 18]) over surfaces coated with motor proteins.[3] To actualize the utility of such transport systems, it is needed to develop some switching systems allowing the control of their motility. Especially, a complete ON/OFF switching would be necessary in

future applications of natural molecular motors for manipulating nano materials as cargos freely in hand from a desired point to the other at any desired timing.

Higuchi *et al*.[19] used caged ATP as a photocontrolled switch; their inactive caged (motility OFF) state could be converted to an active uncaged (motility ON) state through irradiation with ultraviolet (UV) light. Hess *et al*.[15] also utilized the photolysis of caged ATP to develop light-controlled molecular shuttles on engineered kinesin tracks. They could turn the microtubule motility ON through UV-induced release of ATP and OFF through hexokinase-mediated enzymatic degradation of ATP. However, switching from the ON to OFF state was not possible with desired timing in the above mentioned studies. Uyeda and Tatsu *et al*.[20] demonstrated the switching of kinesin's activity from the ON to OFF state through photolysis of a caged peptide derived from the kinesin C-terminus tail domain, a known inhibitor of the kinesin's motor domain. They demonstrated an 80% decrease in the initial gliding velocity of the microtubules on the kinesin surface after photochemical deprotection of the o-nitrobenzyl protecting group on the caged peptide. Unfortunately, the microtubule gliding did not stop completely at the saturated inhibitor concentration; in addition, recovery of the initial gliding velocity was impossible once inhibited (i.e., this process is irreversible). Martin *et al*.[21] demonstrated an electrically switchable polymer surface involving the polymer poly(CH_2OH-EDOT) being switched from a dedoped (neutral) state to a doped (polycationic) state; the ATPase activity of the adsorbed kinesin decreased reversibly by 35% with a

concomitant decrease in the gliding speed of the kinesin-driven microtubules. Unfortunately, the gliding motility did not come to a complete stop when the surface of the polymer changed from its neutral state to its polycationic state. Ionov *et al*.[22] developed a thermoresponsive polymer, poly(isopropyl acrylamide) (PNIPAM), that repelled the microtubules when the surface was cooled and then re-permitted gliding when upon heating. In that method, temperature-modulation of PNIPAM (between 27 and 35 °C) resulted in reversible unbinding and gliding phenomena; unfortunately, is not suitable for use in a transport system intended for travel between two desired positions because unbinding from the surface led to diffusion of microtubules into the solution.

Recently, our group has made significant findings regarding regulation of the gliding velocity of microtubules on kinesin through exploitation of the photoresponsive behavior of azobenzenes.[23-27] We have demonstrated dynamic photocontrol of kinesin-driven microtubule motility through use of a photoisomerizable monolayer surface[28] presenting amino acids with terminal amino groups. Using a lysine- or arginine-functionalized azobenzene monolayer surface, we could control the gliding velocity of microtubules on kinesin, but with only a 15% difference in velocity, upon repeated *cis–trans* isomerizations. We have also achieved upto 79% difference in gliding velocity of microtubules on kinesin when using azobenzene-containing energy molecules[29, 30] which can

be used instead of ATP. We failed to completely stop the gliding motility because of the limitations of azobenzene isomerization: the 8% of the *trans* isomer remaining in the UV photostationary state (PSS) could still provide the energy required to drive the motility. All the methods described above suffer from various limitations that disrupt the gliding motility of microtubules in a fully reversible manner. The challenge has remained to develop a system capable of perfect ON/OFF switching of motility with complete control over timing.

In this dissertation we investigated the photoresponsive inhibition properties of azobenzene-tethered peptides for the regulation of kinesin-microtubule motility. we have discovered a compound containing a peptide and a terminal azobenzene unit that completely stops and starts the motility of kinesin-microtubule in its *trans* and *cis*-rich states, respectively, obtained after irradiation with visible and UV light, respectively. A gliding motility system utilizing this photoresponsive inhibitor allowed *in situ* control and spatiotemporal control over the motion of microtubules on a kinesin-coated glass substrate. The rapid and repeatable regulation of such motility suggests that this system has great potential for use in the development of nano transport systems.[7–12]

2. EXPERIMENTAL SECTION

2.1 Materials

4-(Phenylazo)benzoic acid, Nova PEG Rink amide resin, Fmoc-Ser(t-Bu)alkoresin, Fmoc-Arg(pmc)alkoresin, F-moc–protected amino acids [Fmoc-Ala-OH, Fmoc-Arg(Pmc)-OH, Fmoc-Gln(Mbh)-OH, Fmoc-Gly-OH, Fmoc-His(Boc)-OH, Fmoc-Ile-OH, Fmoc-Lys(Boc)-OH, Fmoc-Pro-OH, Fmoc-Ser(tBu)-OH], coupling reagents, and solvents were purchased from Watanabe Chemical, Tokyo Chemical Industries, and Wako Pure Chemicals and used without further purification. Peptide-grade dimethylformamide (DMF) and dichloromethane (DCM) were used for elongation of the amino acids. High-performance liquid chromatography (HPLC)–grade acetonitrile and milli-Q water were used for purification of peptide samples.

2.2 General methods, instrumentation and measurements

All peptides were synthesized using a Burrel Wrist action Shaker-Model 75. Peptide purification and analysis were performed using Shimadzu reversed-phase (RP) HPLC systems. Pure peptide fractions from HPLC were freeze-dried using an EYELA FDU-2200 lyophilization system. Matrix assisted laser desorption ionization time-of-flight mass spectrometry (MALDI-TOF MS) was performed on an applied Biosystems Voyager-DE pro instrument with positive-ion mode. Absorption spectra were recorded using an Agilent 8453 single-beam spectrophotometer and a Hitachi U-3100 absorption spectrophotometer.

Photoisomerization studies were conducted using a Hg/Xe lamp after passage through appropriate filters (365 or 436 nm).

2.3 Synthesis

2.3.1 General procedure for the elongation of amino acid sequences through Fmoc solid phase peptide synthesis (SPPS)

Diisopropyl ethyl amine (DIPEA) (8 equiv) was added to a solution of Fmoc-protected amino acid (4.0 equiv), 1-hydroxy-1H-benzotriazole monohydrate (HOBt, 4.0 equiv) and O-(Benzotriazol-1-yl)-N,N,N,N-tetramethyluronium hexafluorophosphate (HBTU, 4.0 equiv) in DMF. The solution was pre-activated for 1 min and then transferred to a reaction vessel containing the pre-swelled resin (0.52 mmol/g) and subjected to shaking for 60 min at 25 °C. The resin was then washed thoroughly with DMF (3 × 4 mL), DCM (3 × 4 mL), and DMF again (3 × 4 mL). A solution of 20% piperidine in DMF (4 mL) was added and then the mixture was subjected to shaking for 30 min to remove the N-terminal Fmoc protecting group. The resin was again washed with DMF and DCM as before. To confirm completion of the reactions, color tests (Kaiser tests for free amines; “positive,” violet; “negative,” yellow) was performed using one or two resin beads after each amino acid coupling and also after deprotection of the Fmoc protecting group.

1: H-**RG HSA QIA KPI RPG QHP AAS**-NH_2

2: H-**RG HSA QIA KPI RPG QHPAAS**

3: H-**SAA PHQ GPR IPK AIQ ASH GR**

Scheme 1. Structure of plain inhibitory peptide sequences (Compound **1-3**)

2.3.2 Synthesis of azobenzene-peptides

DIPEA (8 equiv) was added to a solution of 4-(phenylazo)benzoic acid (4.0 equiv), HOBt (4.0 equiv), and HBTU (4.0 equiv) in DMF. The solution was pre-activated for 1 min and then introduced into the reaction vessel soon after deprotection of the Fmoc group from the last amino acid of the peptide sequence. The solution was subjected to shaking for 1.5 h at 25 °C and then the resin was washed with DMF and DCM as described above. This coupling process was performed twice to achieve adequate coupling and relatively good yield. Finally, the azobenzene-peptide was cleaved from the resin through shaking in a solution of reagent-K (TFA/phenol/thioanisole/H_2O/TIPS, 8.25:0.5:0.5:0.5:0.25; 3 mL) for approximately 2 h at 25 °C. After filtration, the crude product was precipitated in cold diethyl ether and centrifuged 2–3 times to remove residual TFA and scavengers. The crude sample was air-dried, dissolved in a suitable amount of solvent, and purified through preparative RP-HPLC.

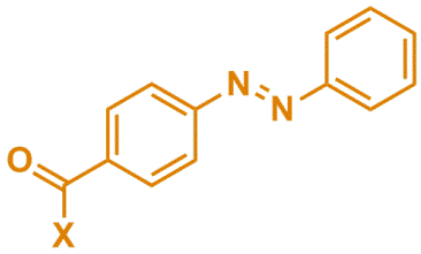

4: X=**RG HSA QIA KPI RPG QHP AAS**-NH_2
5: X=**RG HSA QIA KPI RPG QHP AAS**
6: X=**SAA PHQ GPR IPK AIQ ASH GR**
7: X=**SAA PHQ GPR**
8: X=**IPK AIQ ASH GR**
9: X=**ASH GR**

Scheme 2. Structure of azobenzene tethered inhibitory peptide sequences (Compound **4-9**)

2.4 Characterization

The purity of all the plain peptides and azobenzene-peptides was confirmed using an analytical RP-HPLC system [column: 5C18-MS-II, 4.6 × 250 mm (Waters); eluent: CH_3CN/H_2O containing 0.1% TFA; solvent gradient: 10–35% for plain peptides and 20–45% for azobenzene-peptides, over 1 h; flow rate: 1 mL/min at 25 °C; injection volume: 20 µL; monitoring wavelength: 220 nm for plain peptides, 283 nm (isosbestic point) for azobenzene-peptides)]. The molecular weights of all the peptides were determined using MALDI-TOF MS

2.4.1 HPLC profile of compounds (1-9)

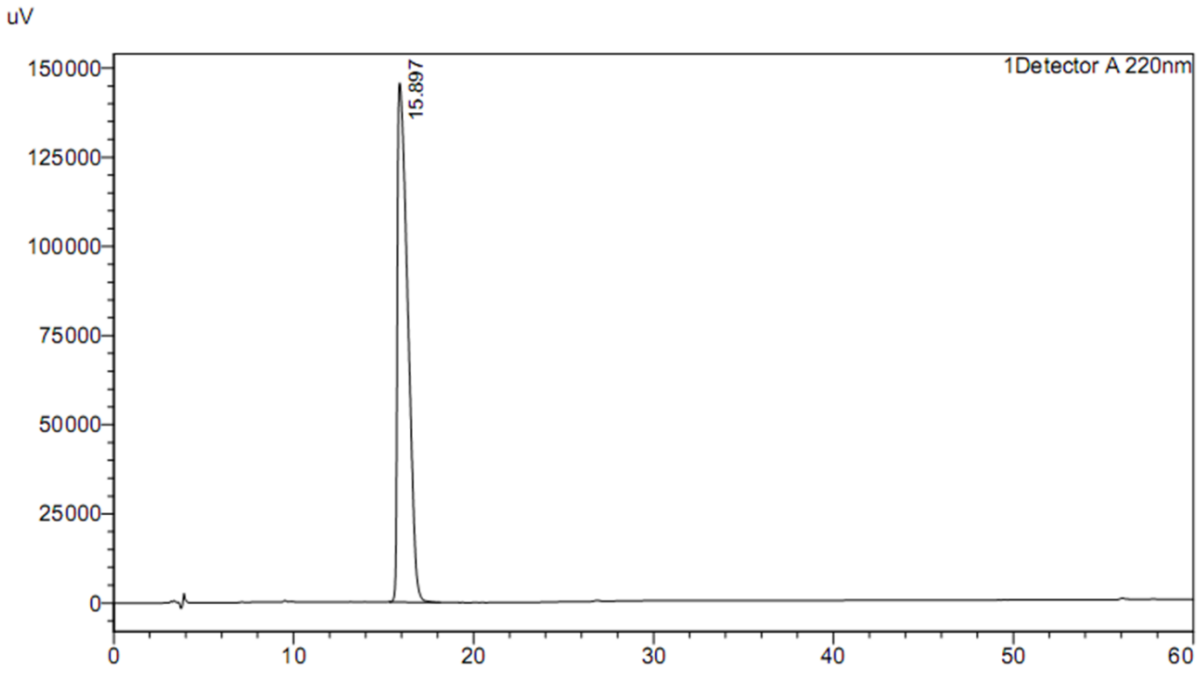

Figure 1. HPLC chromatorgram showing >95% purity of compound **1**

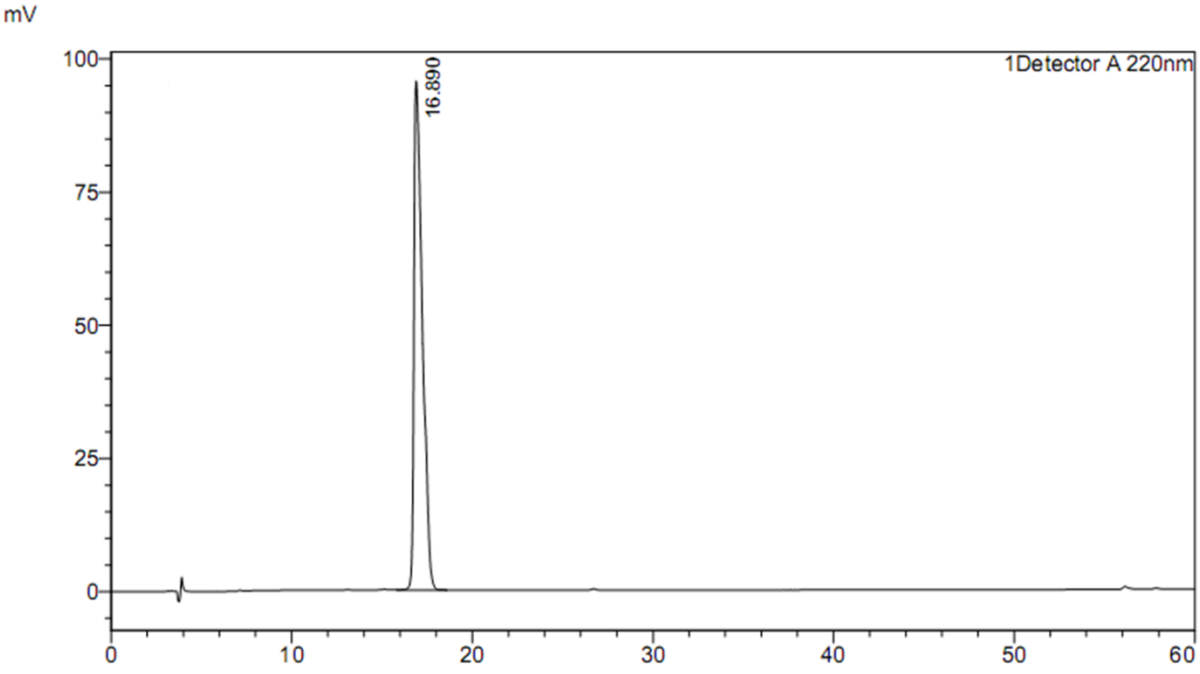

Figure 2. HPLC chromatorgram showing >95% purity of compound **2**

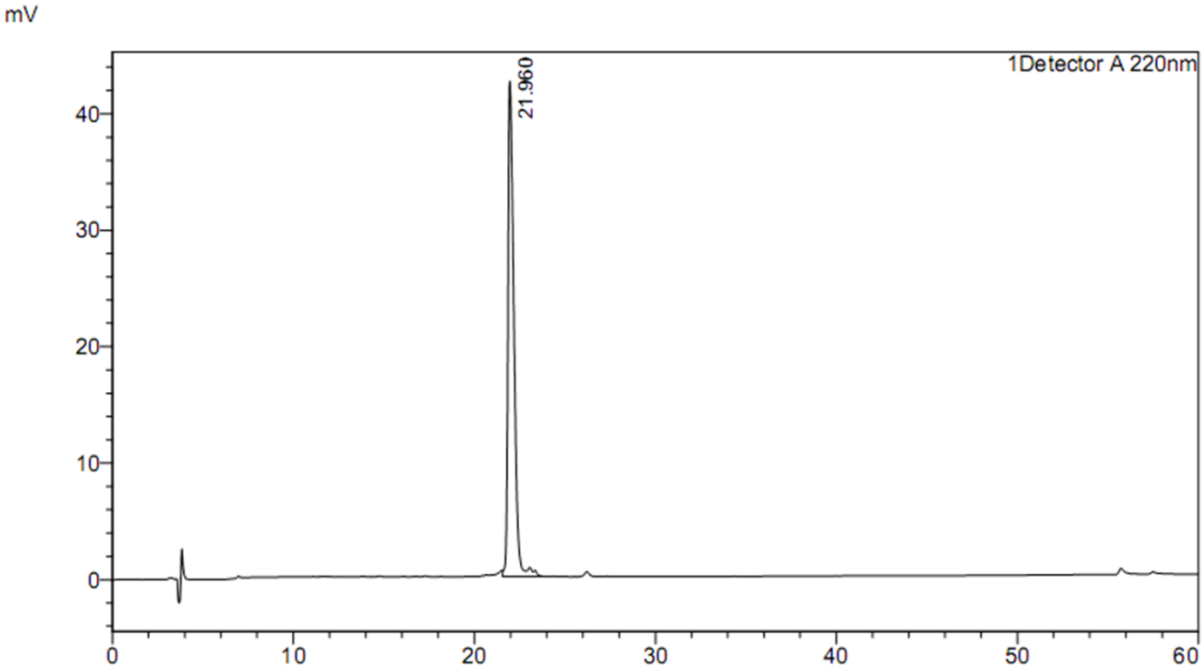

Figure 3. HPLC chromatorgram showing >95% purity of compound **3**

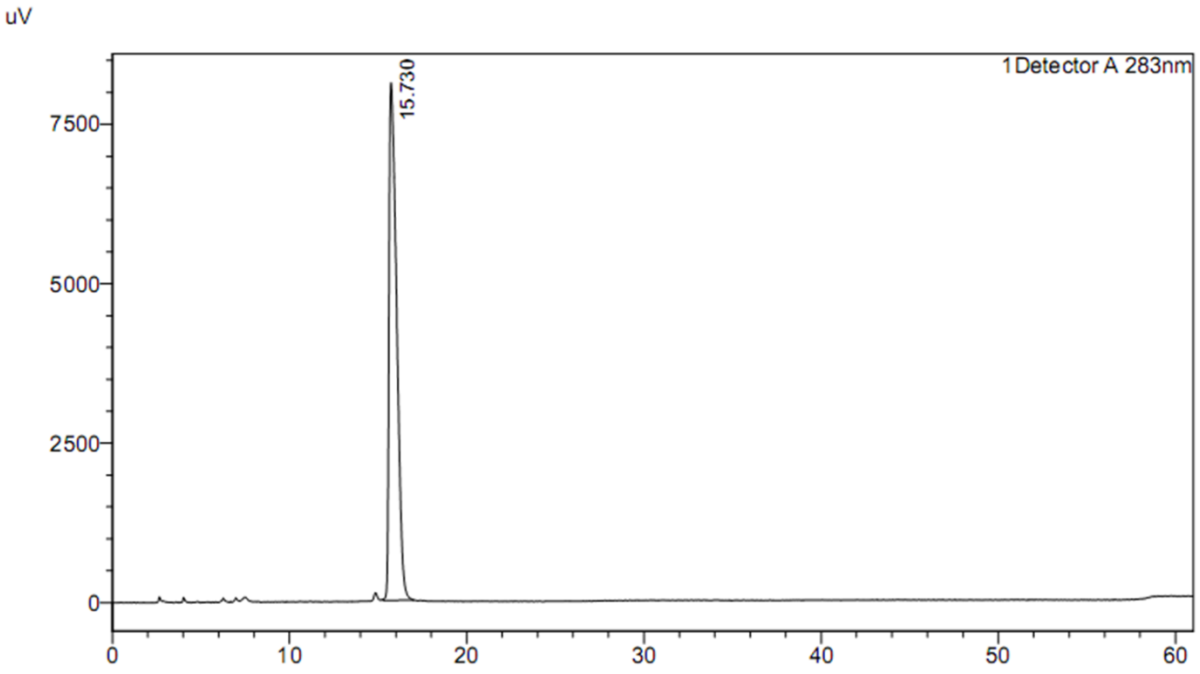

Figure 4. HPLC chromatorgram showing >95% purity of compound **4**

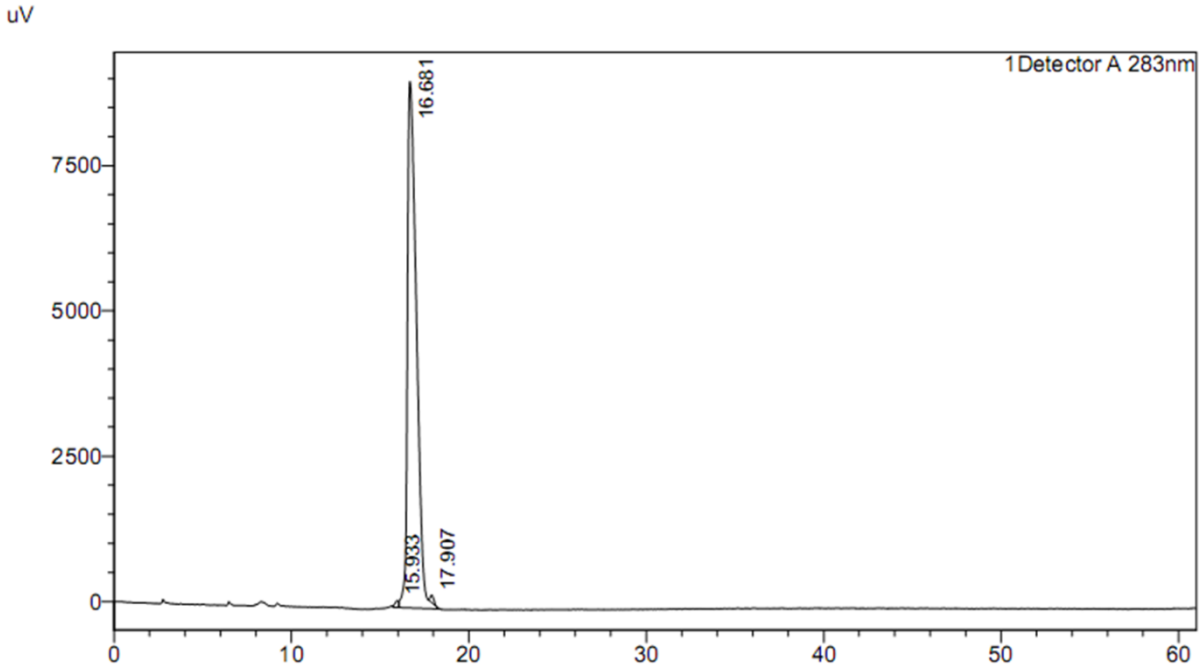

Figure 5. HPLC chromatorgram showing >95% purity of compound **5**

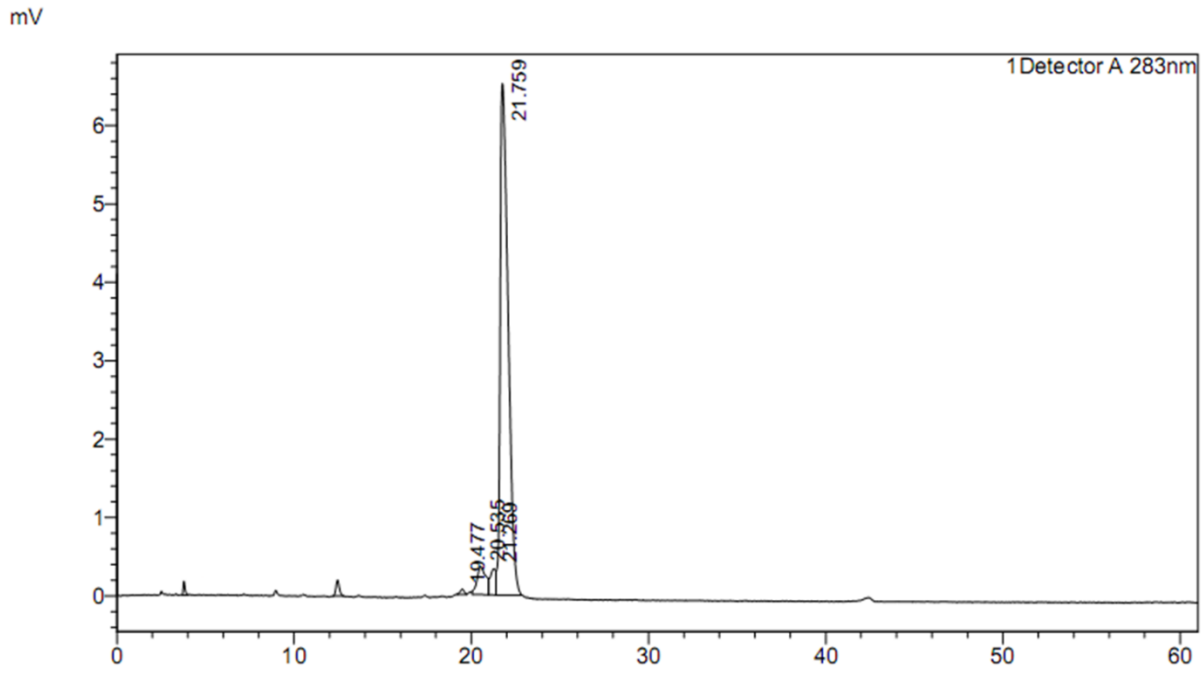

Figure 6. HPLC chromatorgram showing >95% purity of compound **6**

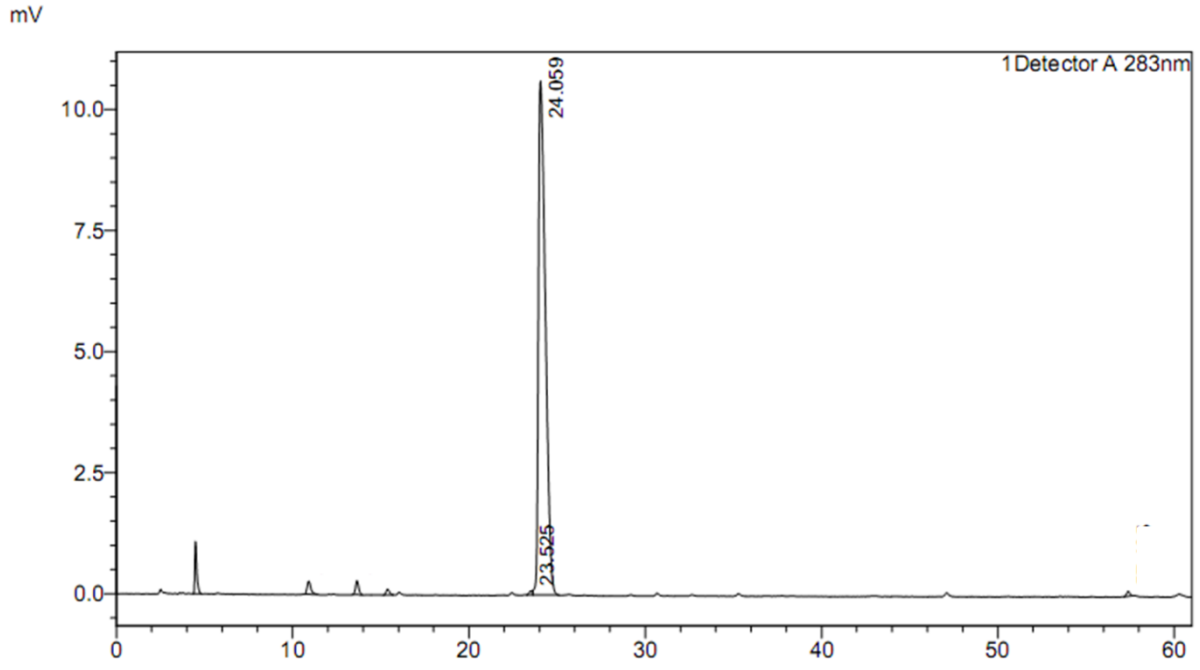

Figure 7. HPLC chromatorgram showing >95% purity of compound **7**

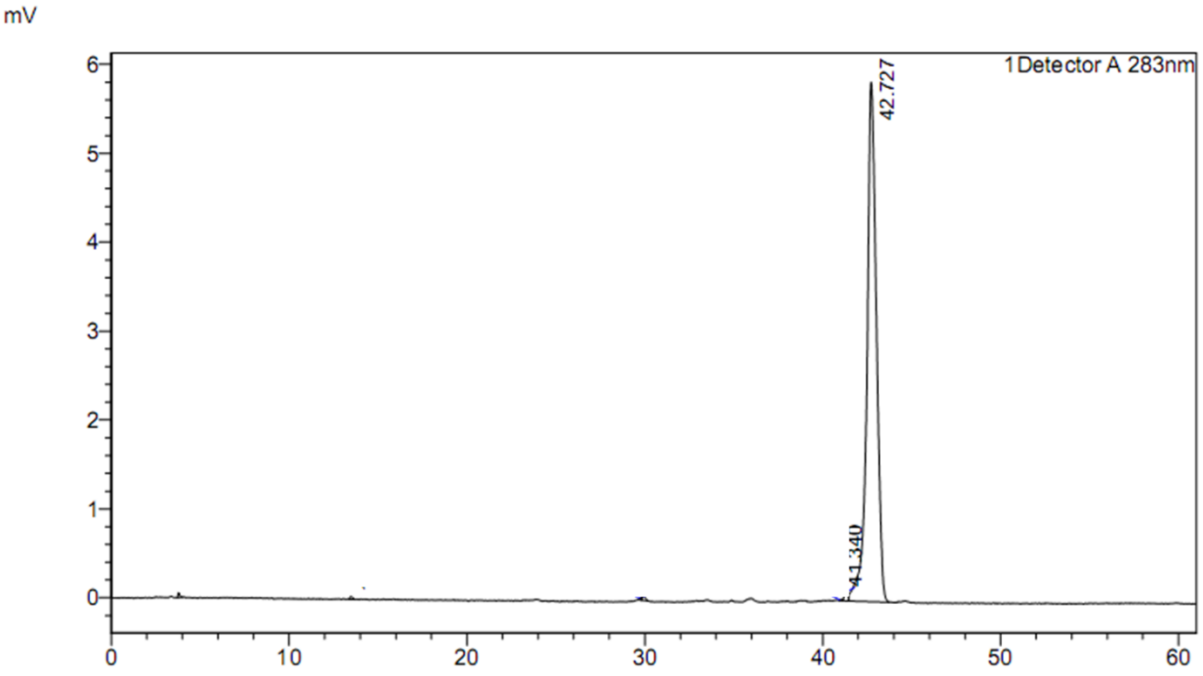

Figure 8. HPLC chromatorgram showing >95% purity of compound **8**

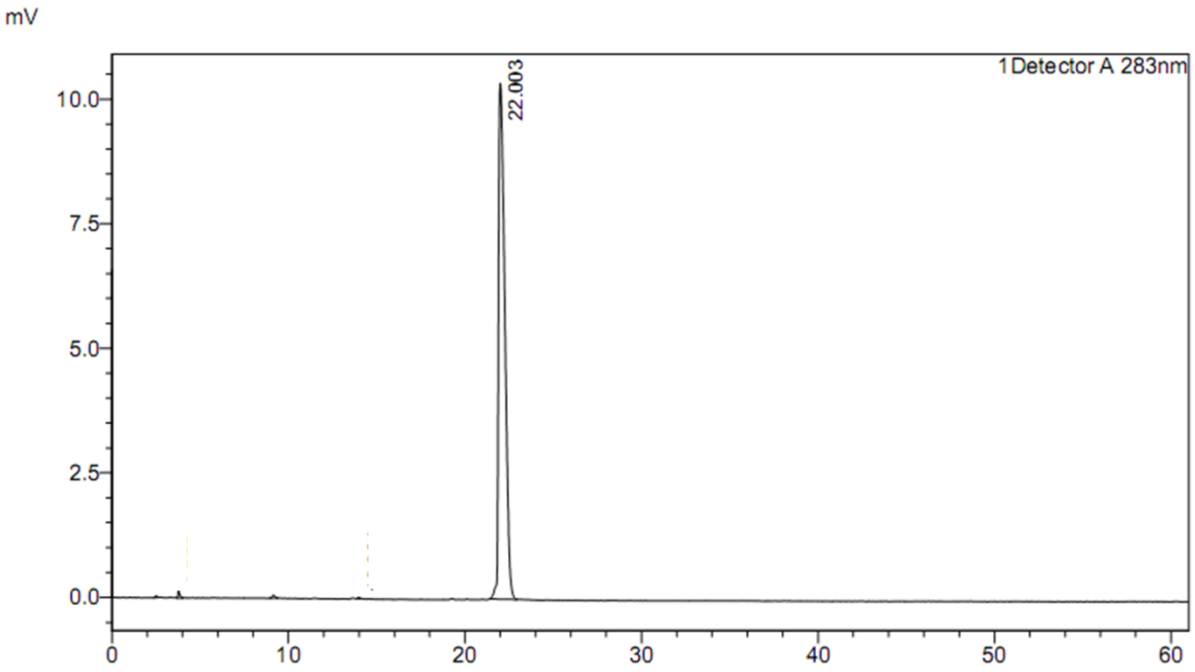

Figure 9. HPLC chromatorgram showing >95% purity of compound **9**

2.4.2 MALDI-TOF Mass spectra of compounds (1-9)

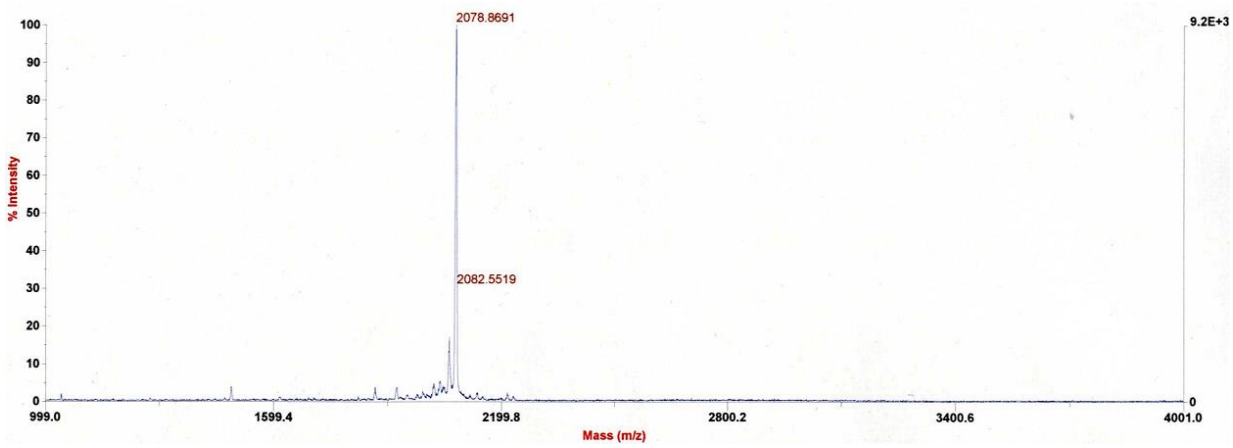

Figure 10. MALDI-TOF Mass spectra of compound **1**: *m/z*=2078.86 $[M+H]^+$ (calcd. 2078.14)

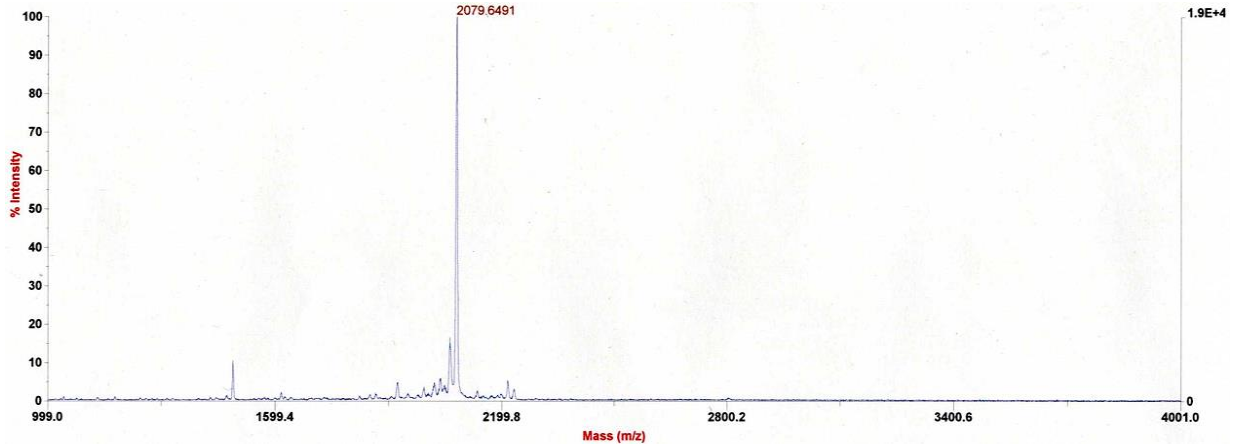

Figure 11. MALDI-TOF Mass spectra of compound **2**: *m/z*=2079.64 $[M+H]^+$ (calcd. 2079.12)

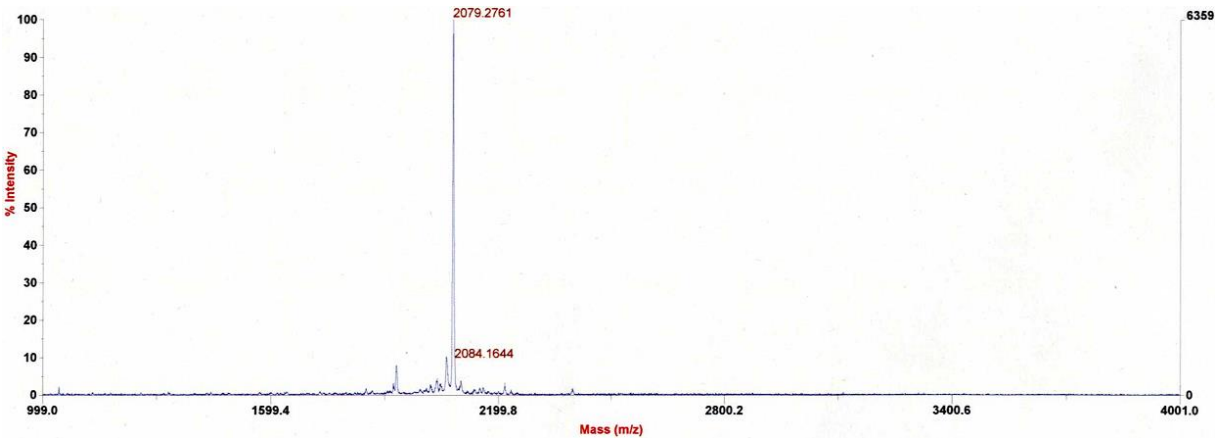

Figure 12. MALDI-TOF Mass spectra of compound **3**: *m/z*=2079.27 $[M+H]^+$ (calcd. 2079.12)

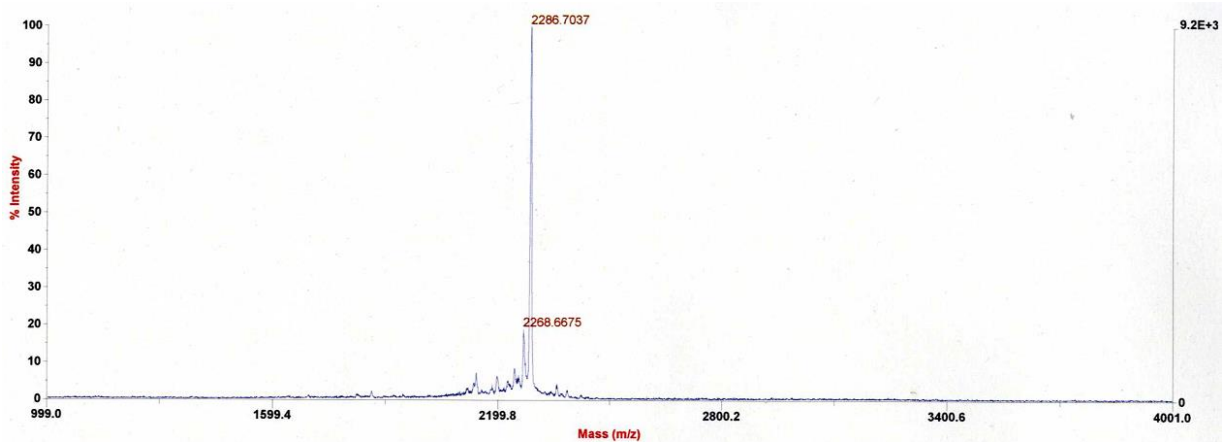

Figure 13. MALDI-TOF Mass spectra of compound **4**: *m/z*=2286.70 $[M+H]^+$ (calcd. 2286.20)

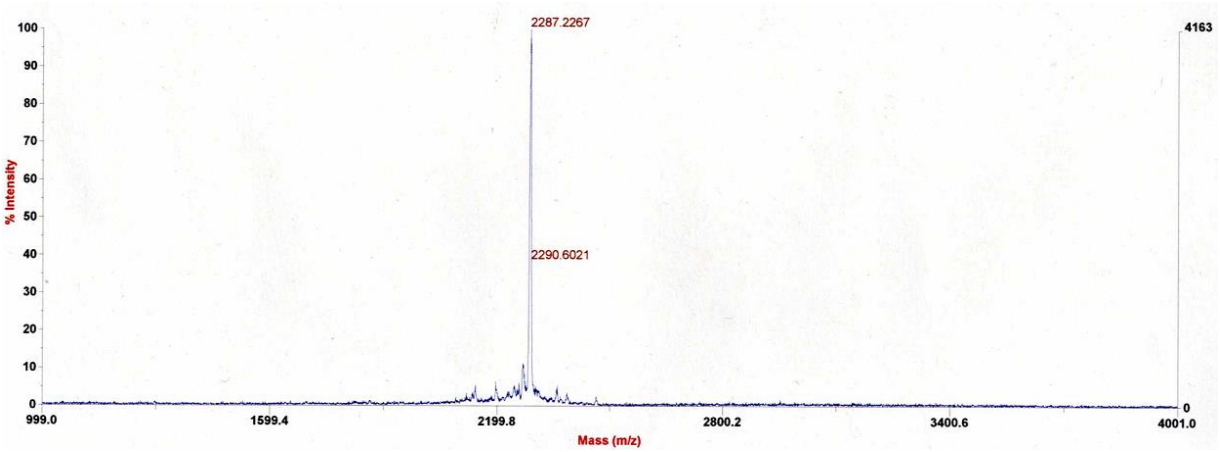

Figure 14. MALDI-TOF Mass spectra of compound **5**: *m/z*=2287.22 $[M+H]^+$ (calcd. 2287.19)

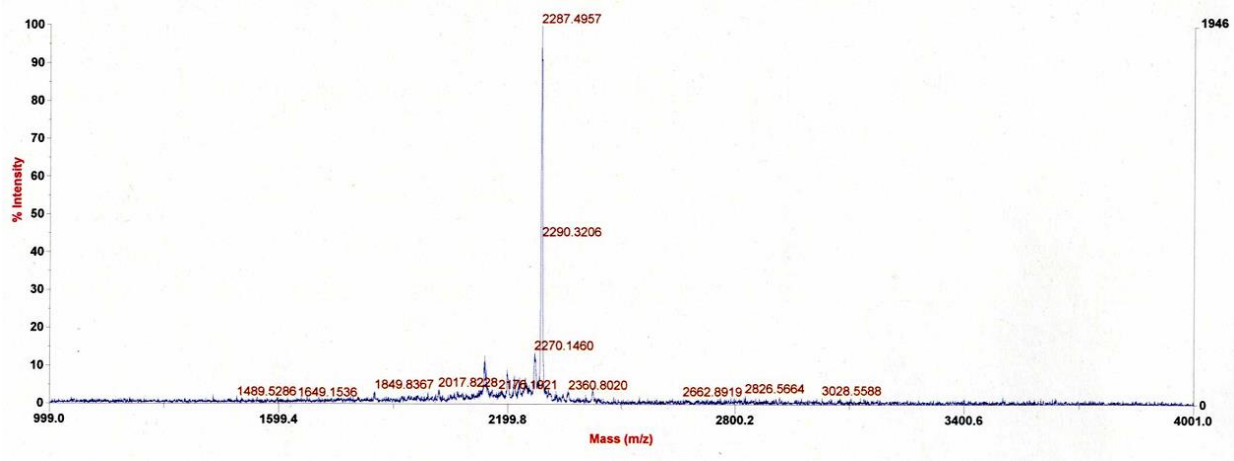

Figure 15. MALDI-TOF Mass spectra of compound **6**: *m/z*=2287.49 $[M+H]^+$ (calcd. 2287.19)

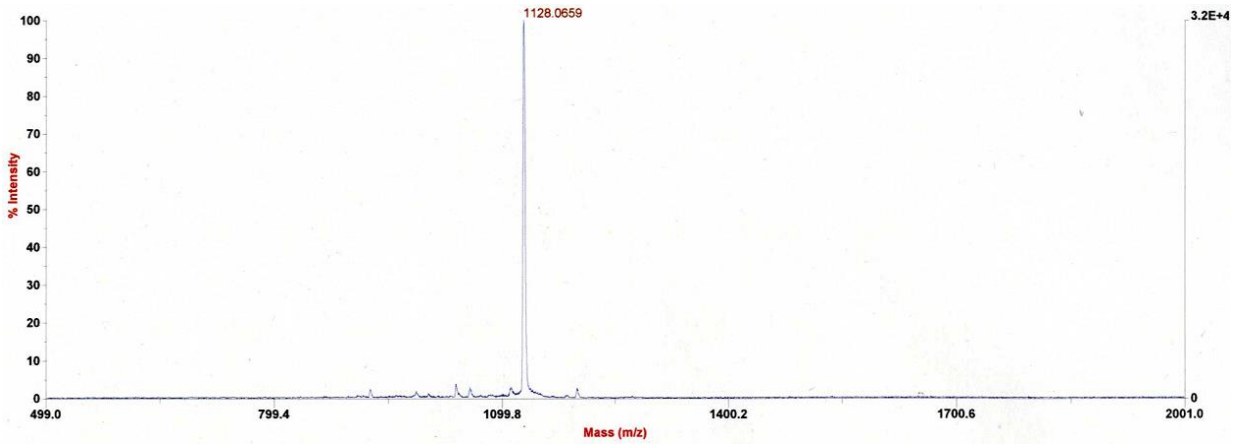

Figure 16. MALDI-TOF Mass spectra of compound **7**: *m/z*=1128.06 $[M+H]^+$ (calcd. 1128.53)

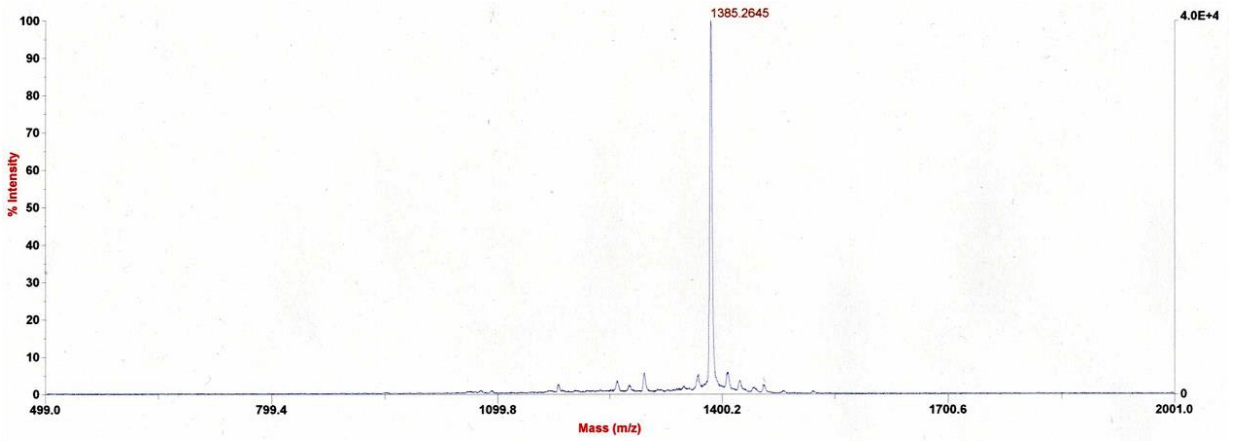

Figure 17. MALDI-TOF Mass spectra of compound **8**: *m/z*=1385.26 $[M+H]^+$ (calcd. 1385.74)

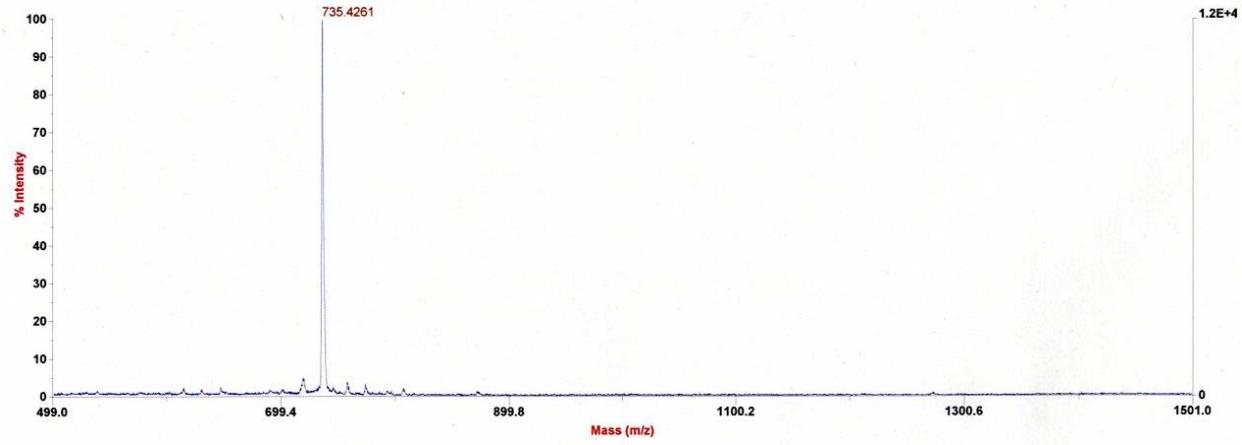

Figure 18. MALDI-TOF Mass spectra of compound **9**: *m/z*=735.42 $[M+H]^+$ (calcd. 735.32)

2.5 Protein purification and preparations

Tubulins were purified from porcine brains through two cycles of polymerization/depolymerization processes in the presence of a high-molarity PIPES buffer. Microtubules (MTs) were polymerized using the purified tubulins and labeled with CF™ 633 succinimidyl ester. The kinesin employed in this study was a recombinant kinesin consisting of 573 amino acid residues from the N-terminus of a conventional human kinesin. This recombinant kinesin fused with His-tag at the N-terminus (plasmid; pET 30b) was expressed in E. coli Rossetta (DE3)pLysS and purified through the general method utilizing Ni-NTA-agarose.

2.6 *In vitro* kinesin-microtubule motility assay

Microtubule motility assays were performed using a fluorescence optical microscope (Olympus BX50) equipped with a UPlan F1 100x/1.30 oil C1 objective lens (Olympus), appropriate filters [630 nm excitation filter; neutral density filter (ND-25, 25% transmission)], an EBCCD color video camera (Hamamatsu C7190), and an Metamorph image processing system (Molecular devices). A Hg/Xe lamp was used as a source of UV and visible light after passage through appropriate filters (365 and 436 nm, respectively). The flow cell chamber for microscopic observation was prepared by taping a cover slip (18 × 18 mm) and a glass slide (76 × 26 mm) together at both extremities to make a flow path (ca. 2 × 18 mm). The kinesin solution containing casein (3.0

μL; kinesin: ca. 0.1 mg/mL; casein: 0.5 mg/mL) was flowed into the prepared chamber and incubated for 3 min. The fluorescently labeled MTs solution (3.0 μL; MTs calculated as tubulin dimer, 0.5 μM; taxol, 10 μM) was then flowed into the chamber and incubated for 3 min, followed by washing with the assay buffer (BRB-40 buffer: PIPES, 40 mM; $MgCl_2$, 2 mM; EGTA, 1 mM) containing taxol (10 μl; 10 μM). After final washing with an assay buffer containing taxol (3.0 μL), an added oxygen scavenger system (casein, 0.5 mg/mL; 2-mercaptoethanol, 0.14 M; glucose, 20 mM; catalase, 20 μg/mL; glucose oxidase, 100 μg/mL; ATP, 1.0 or 0.1 mM), and a desired concentration of plain inhibitory peptide or azobenzene-tethered inhibitory peptide, the flow cell chamber was subjected to fluorescence microscopic observation with the image recorded for 40 s. Furthermore, the chamber was removed and irradiated with UV at ca. 28 mW/cm^2 (40 s) or visible light at ca. 25 mW/cm^2 (40 s) to attain the respective PSS. Again, the chamber was returned to the microscope for observation and recording as before. The recorded video images were analyzed using ImageJ software. The velocity of the microtubules was obtained from the average of 10 measurements (abnormal microtubules, which were partially attached or detached, waved; they were excluded from the measurement). The motility assays were performed at 23 °C.

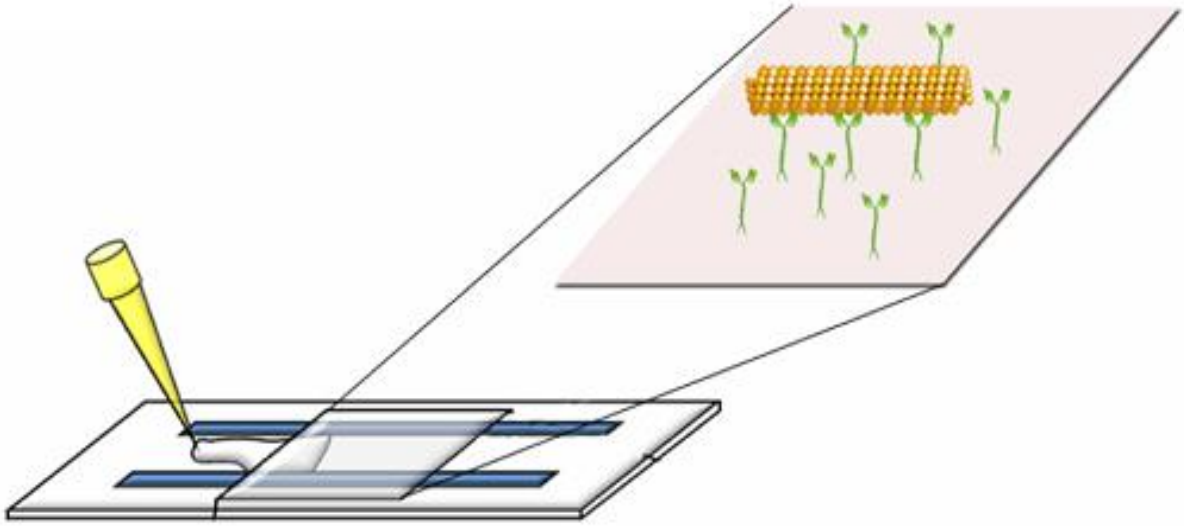

Figure 19. Schematic diagram of the *in vitro* kinesin-microtubule motility assay system.

2.7 *In situ* control of gliding velocity of microtubules

In situ control of the gliding velocity of microtubules was demonstrated using compound **8** on an inverted fluorescence optical microscope (Nikon, Ti-E) equipped with a 100×/1.45 NA oil-immersion objective lens (Nikon) and appropriate filters (Chroma, Semrock); images were recorded using a digital CMOS camera (ORCA-Flash 4.0-V2, Hamamatsu) and the HCI Image processing system (Hamamatsu); 635-nm light from a solid laser (RGB laser systems, Mini Las) was used as the excitation light source. A 365-nm light emitting diode (LED, Hamamatsu) and a 436-nm Hg lamp were used as sources of UV and visible light, respectively, transmitted through appropriate filters. The flow cell chamber was prepared as described for the *in vitro* motility assay. The prepared flow cell chamber containing kinesin, microtubules, oxygen

scavengers, ATP (1.0 mM), and compound **8** (2.0 mM) was subjected to microscopic observation and monitoring. *In situ* imaging was performed continuously under excitation with 635-nm light. The flow cell chamber was irradiated with UV at ca. 1 W/cm^2 (1 s) and visible light at ca. 40 W/cm^2 (1 s) alternately during *in situ* imaging to attain the UV and visible PSSs of compound **8**. A video recording of the gliding microtubules was taken continuously for 5 min, including the interval maintaining the UV and visible PSSs (20 s) between each irradiation.

2.8 *In situ* spatiotemporal control over the gliding velocity of microtubules

In situ spatiotemporal control over the gliding velocity of microtubules was demonstrated using compound **8** on an inverted fluorescence optical microscope (Nikon, Ti-E) equipped with a 100×/1.45 NA oil-immersion objective lens (Nikon) and appropriate filters (Chroma, Semrock); images were recorded using a digital CMOS camera (ORCA-Flash 4.0-V2, Hamamatsu) and the HCI Image processing system (Hamamatsu); 635-nm light from a solid laser (RGB laser systems, Mini Las) was used as the excitation light source. A 365-nm light emitting diode (LED, Hamamatsu) and a 436-nm Hg lamp were used as sources of UV and visible light, respectively, transmitted through appropriate filters. The flow cell chamber was prepared as described for the *in vitro* motility assay. The prepared flow cell chamber containing kinesin, microtubules, oxygen scavengers, ATP (1.0 mM), and compound **8** (2.0 mM) was subjected to

microscopic observation and monitoring. *In situ* imaging was performed continuously under excitation with 635-nm light. A selected region of the flow cell chamber was irradiated with 436 nm light at ca. 16 W/cm^2 through the objective lens from the bottom. At the same time, the whole area of the flow cell including the 436 nm light irradiating region was exposed to 365 nm light at ca. 300 mW/cm^2 from the top continuously to attain respective PSSs of compound **8** (Figure 20). A video recording of the gliding microtubules was taken continuously for more than 10 min.

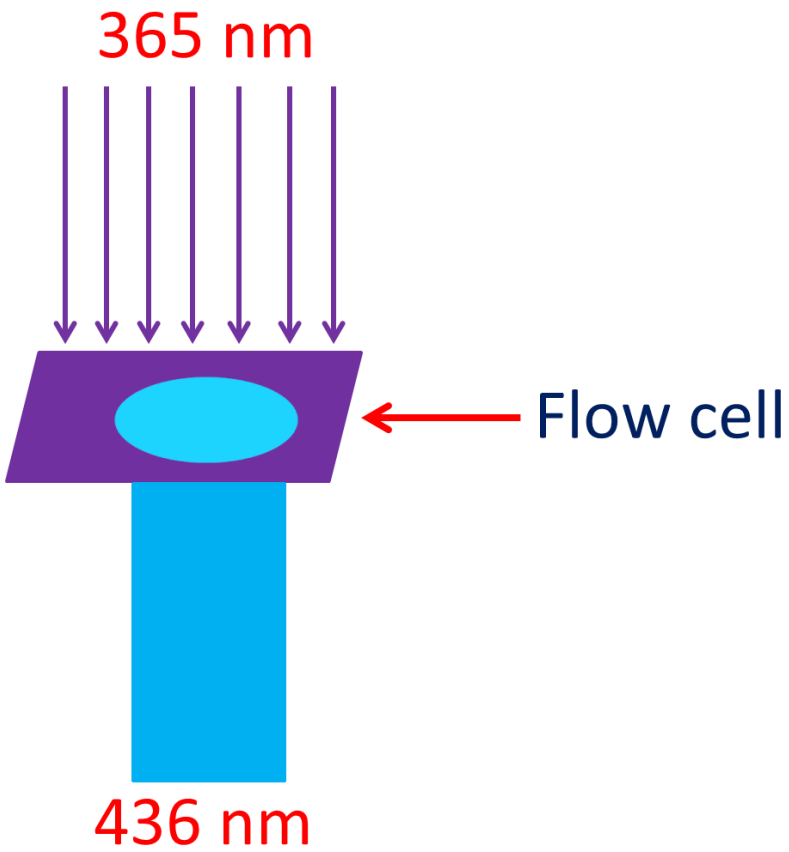

Figure 20. Schematic diagram illustrates the light irradiation for the *in situ* spatiotemporal control of the gliding velocity of microtubules.

2.9 ATPase assay

In the presence of azobenzene-peptide **8** and microtubules, the kinesin ATPase activity was measured using a simple, sensitive colorimetric assay based on determination of released inorganic phosphate ions by an improved malachite green procedure. In short, at fixed time intervals, aliquots (5 μL) were removed from the motility solution containing kinesin (ca. 0.1 mg/mL), microtubule (0.5 μM for tubulin dimer), ATP (1mM) and **8** (2mM) in flow cells and quickly mixed with an equal volume of ice-chilled perchloric acid (PCA, 500 μL) and malachite green reagent (500 μL). The mixture was kept at 25 °C for 35 min and then the absorbance was measured at 630 nm using an absorption spectrophotometer; the rate of Pi release was determined. Experiments were performed for both non-irradiated and 365-nm irradiated (40 s) flow cells to determine the rates of release of Pi in the *trans* and *cis*-rich states.

3. RESULTS AND DISCUSSION

3.1 Synthesis, photoisomerization and thermal stability of azobenzene-peptides

It has been reported previously that the kinesin C-terminus tail domain suppresses the ATPase activity of the motor domain of kinesin.[31–33] Uyeda and Tatsu *et al*.[34] reported that 20- and 30-mer peptides derived from the kinesin C-terminus tail domain effectively inhibit the kinesin-microtubule motility; they also demonstrated photocontrol over the kinesin-microtubule motility by preparing caged peptides having these amino acid sequences.[20] It was possible to decrease the inhibition effect of the peptide by protecting the amino group of the lysine residue with an o-nitro benzyl group, which is cleavable upon irradiation with UV light. Our aim was to regulate the motion of microtubule gliding on kinesin in a fully reversible manner by developing a novel photoswitchable inhibitor. To do so, we selected a previously reported 20-mer amino acid sequence (compound **1**, Scheme 1) as the first candidate for the inhibitory peptide unit. We appended a photoisomerizable azobenzene unit to its N-terminus to obtain compound **4** (Scheme 1). We synthesized compounds **1** and **4** separately through Fmoc solid phase peptide synthesis, purified them using HPLC and characterized by mass spectrometry.

(a) Plain Inhibitory Peptides :

1: H-**RG HSA QIA KPI RPG QHP AAS**-NH_2

2: H-**RG HSA QIA KPI RPG QHPAAS**

3: H-**SAA PHQ GPR IPK AIQ ASH GR**

(b) Photoresponsive Inhibitory Peptides :

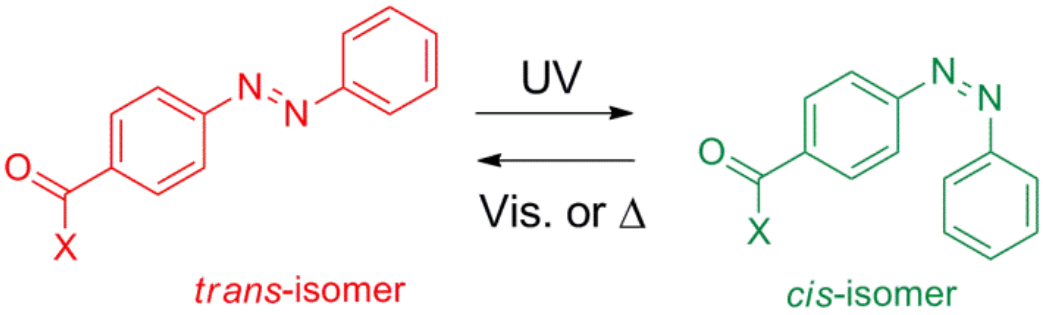

4: X=**RG HSA QIA KPI RPG QHP AAS**-NH_2

5: X=**RG HSA QIA KPI RPG QHP AAS**

6: X=**SAA PHQ GPR IPK AIQ ASH GR**

7: X=**SAA PHQ GPR**

8: X=**IPK AIQ ASH GR**

9: X=**ASH GR**

Scheme 1. (a) Plain inhibitory peptide sequences from the kinesin's tail domain (**1**–**3**). (b) The *trans* and *cis* forms of azobenzene-tethered inhibitory peptide sequences from the kinesin's tail domain (**4**–**9**).

Prior to performing the *in vitro* kinesin-microtubule motility experiment,[35] we tested the photoisomerization properties of compound **4** using UV–Vis absorption spectroscopy [Figure 1(a)]. We measured the photoisomerization and thermal stability of compound **4** in BRB-40 buffer solution, the same buffer used for the kinesin-microtubule motility experiments. Upon irradiation of the

solution of compound **4** in its *trans* state with light at 365 nm, the π–π* transition band at 325 nm gradually decreased while the n–π* transition band near 420 nm increased, typical features of the *cis*-rich state of an azobenzene derivative.[36] Upon irradiation of the UV-irradiated solution with light at 436 nm, the n–π* transition band gradually decreased and the π–π* transition band gradually increased, almost returning to the initial absorption spectrum. These absorption spectral changes were repeated for at least 10 cycles without any sign of fatigue [inset to Figure 1(a)]. These results suggest that compound **4** has excellent photoisomerization properties in the buffer solution—a necessary feature for reversible switching of biological functions.[37, 38] HPLC analysis—monitoring at a wavelength of 283 nm, the isosbestic point—revealed the existence of 88 and 80% of the *cis* and *trans* isomers of compound **4**, respectively, at their UV and visible PSSs [Figure 3(a)]. We confirmed the thermal stability of the *cis* isomer at 25 °C through observation of its absorption spectra in the dark [Figure 2(a)]; we observed that only less than 1% of the *cis* isomer isomerized to the *trans* isomer after 1 h, excluding the possibility of the thermal back-reaction occurring during the motility experiments.

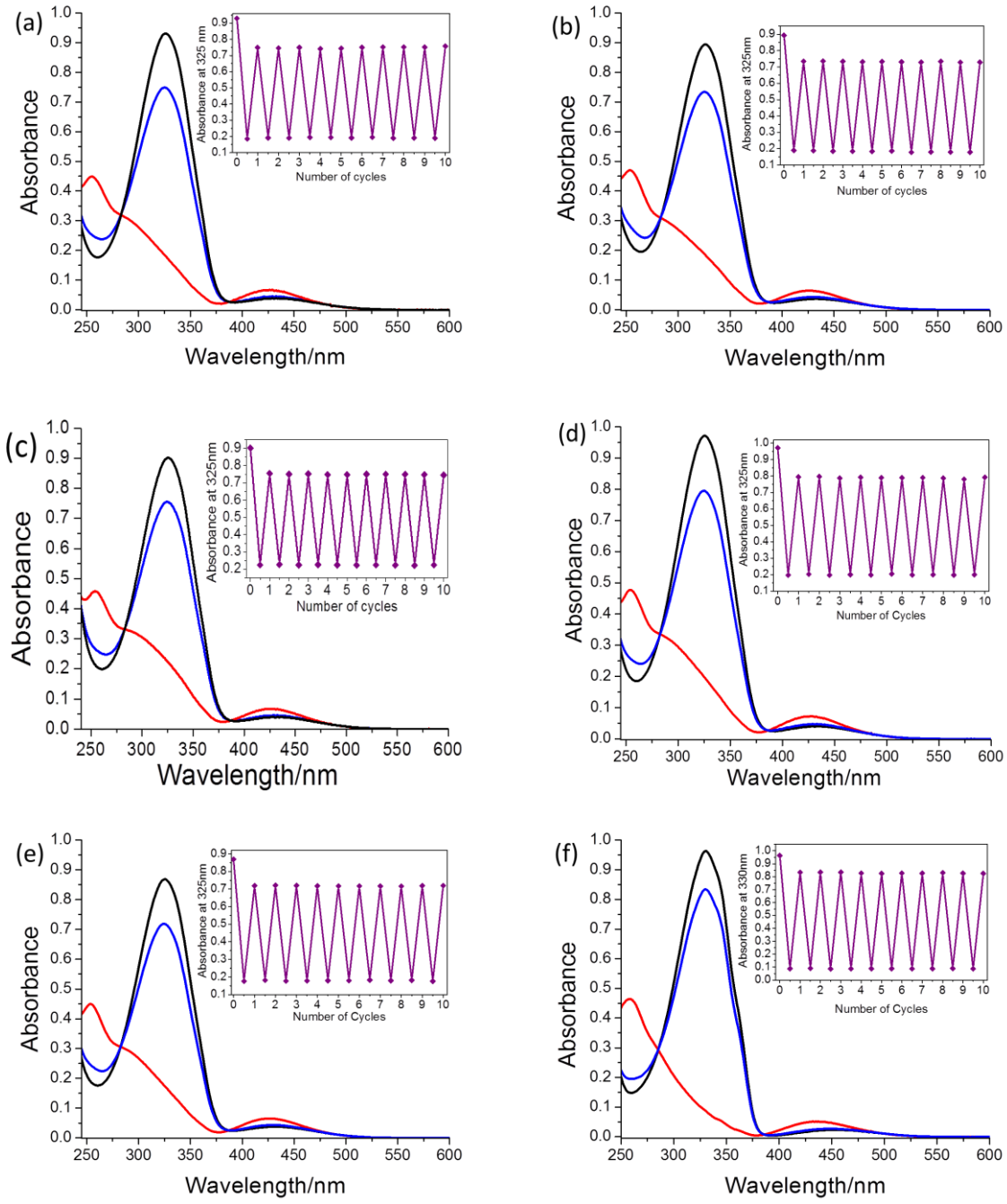

Figure 1. UV–Vis absorption spectra of compounds **4**-**8** (a-e) in BRB-40 buffer solution and **9** (f) in DMSO at 25 °C; before photo-irradiation (black line), PSS under 365-nm irradiation (red line), PSS under 436-nm irradiation (blue line). Inset: Absorbance changes at 325 nm after alternating irradiation at 365 and 436 nm light for 10 cycles.

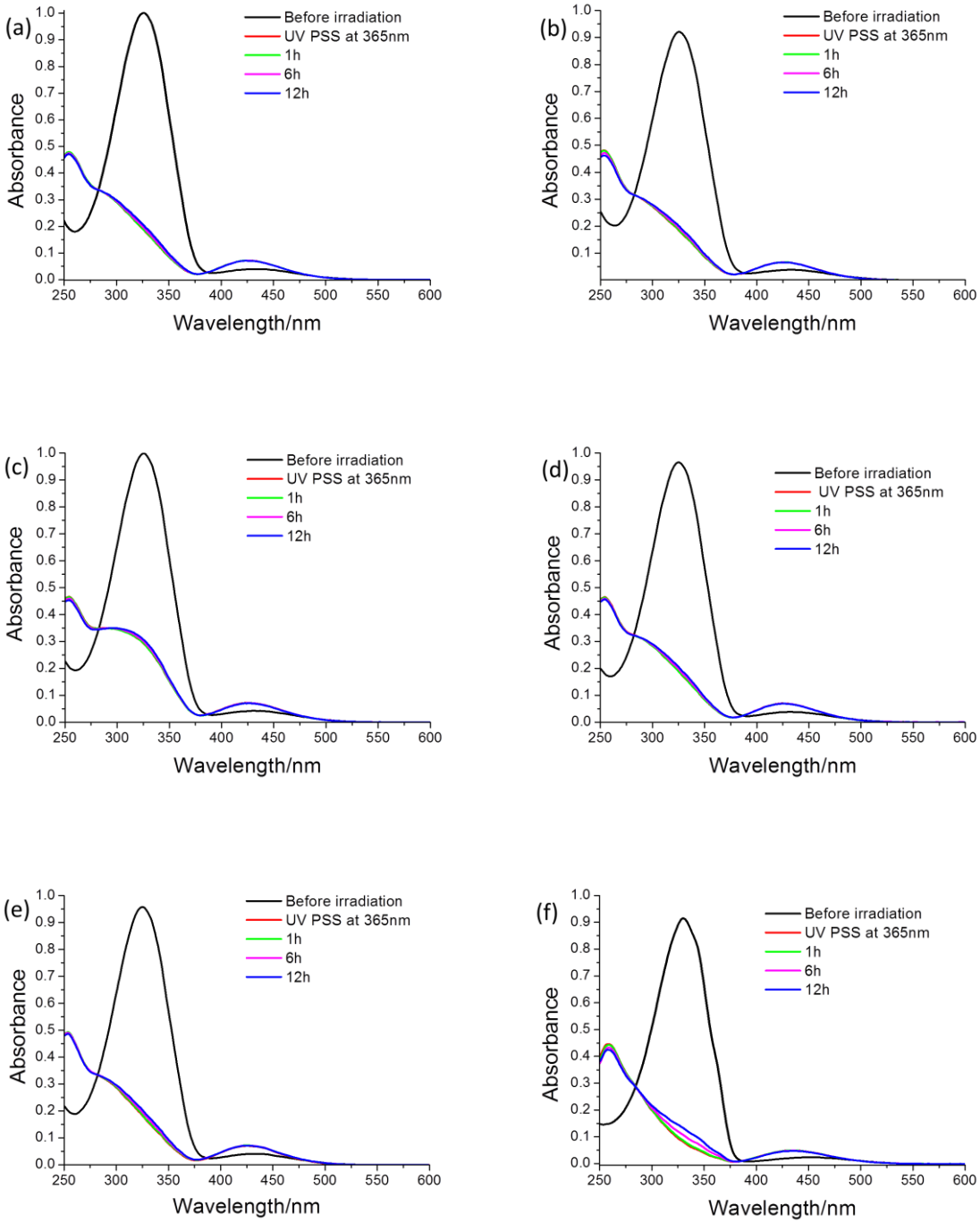

Figure 2. UV-Visible absorption spectra of compounds **4-8** (a-e) in BRB-40 buffer solution and **9** (f) in DMSO after irradiation for 40 s at 365 nm and then incubation in the dark at 25 ^{0}C.

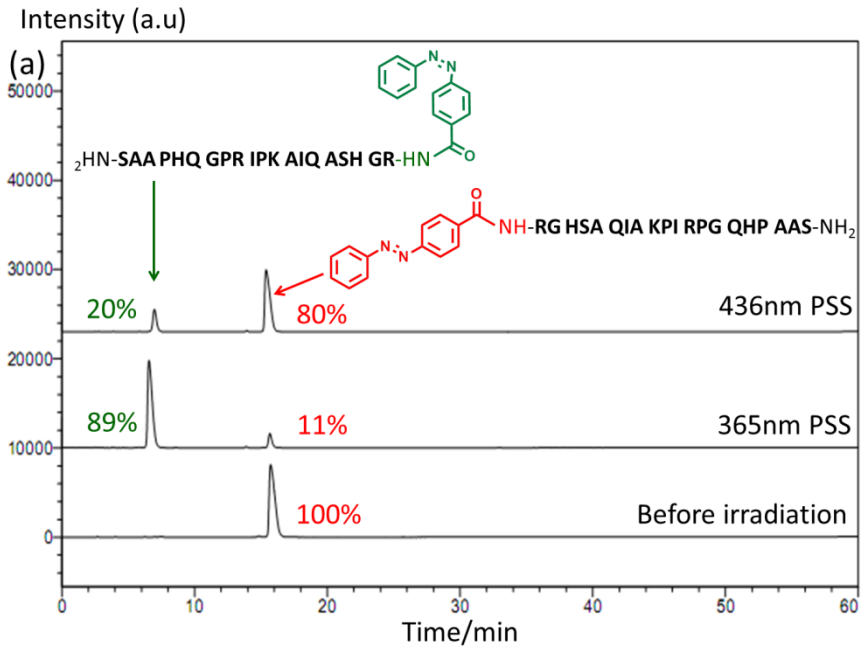

Figure 3a. HPLC chromatogram showing the *cis* and *trans* isomer ratio of compound **4** at before irradiation, after UV and visible PSSs respectively.

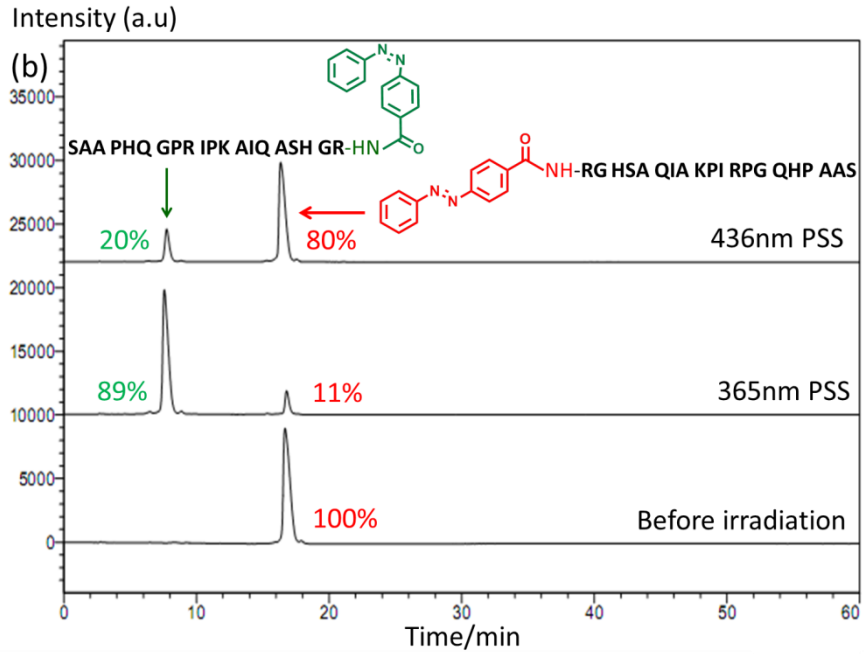

Figure 3b. HPLC chromatogram showing *cis* and *trans* isomer ratio of compound **5** at before irradiation, after UV and visible PSSs respectively.

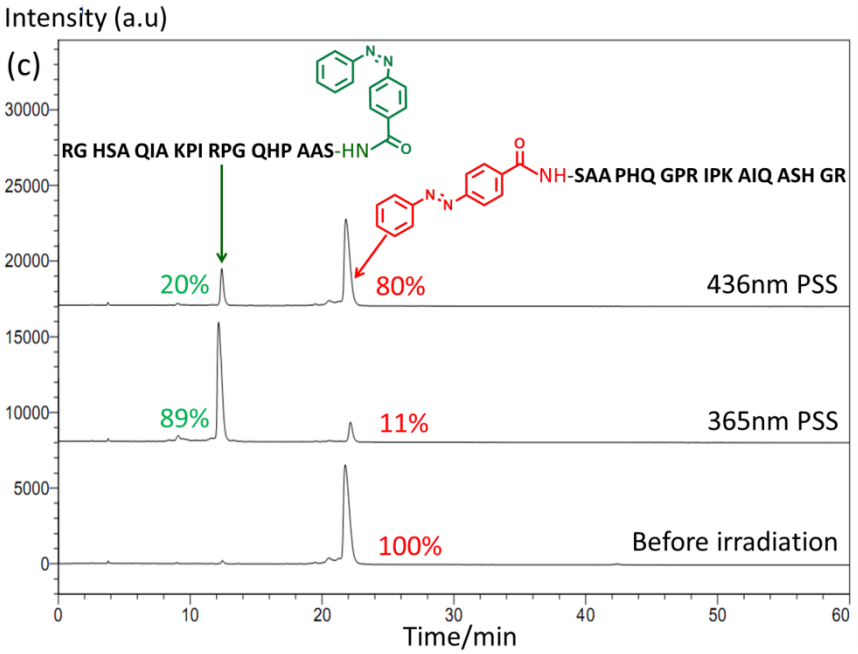

Figure 3c. HPLC chromatogram showing *cis* and *trans* isomer ratio of compound **6** at before irradiation, after UV and visible PSSs respectively.

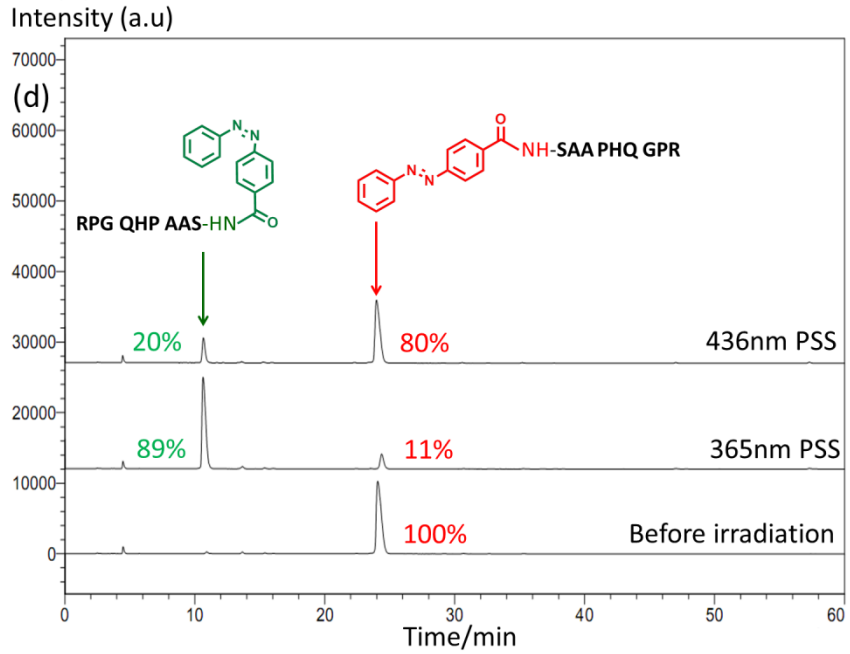

Figure 3d. HPLC chromatogram showing *cis* and *trans* isomer ratio of compound **7** at before irradiation, after UV and visible PSSs respectively.

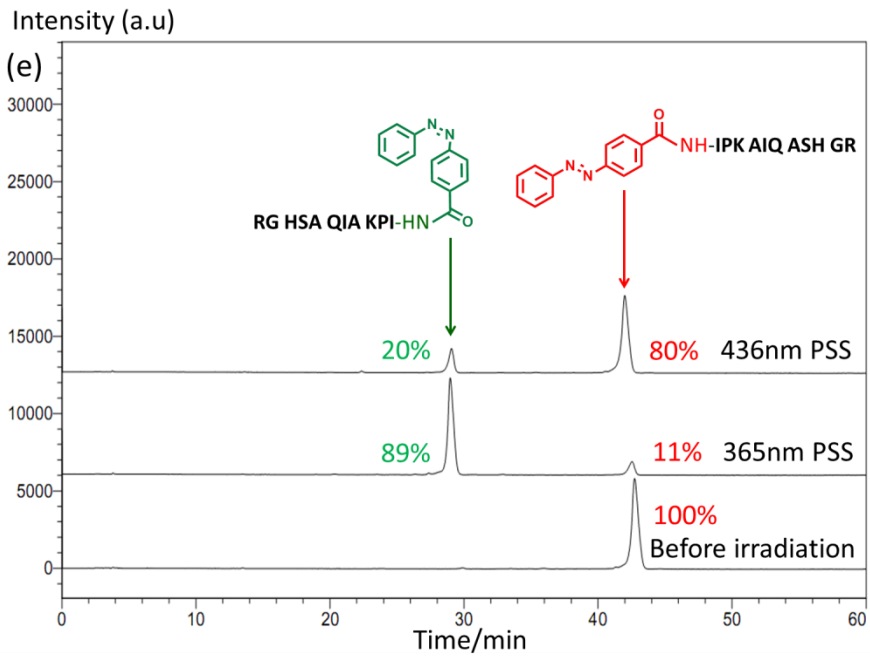

Figure 3e. HPLC chromatogram showing *cis* and *trans* isomer ratio of compound **8** at before irradiation, after UV and visible PSSs respectively.

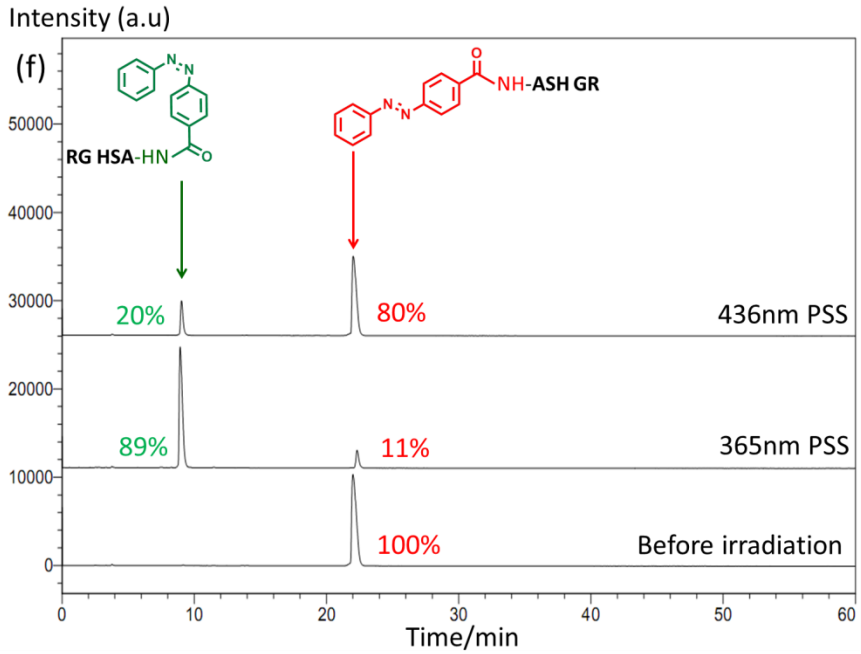

Figure 3f. HPLC chromatogram showing *cis* and *trans* isomer ratio of compound **9** at before irradiation, after UV and visible PSSs respectively.

3.2 Photoswitchability of the motility of kinesin-microtubule by azobenzene-peptides

We evaluated the inhibitory activities of compounds **1** and **4** against kinesin in the presence of 1.0 mM ATP by using a fluorescence optical microscope to monitor the motility of fluorescently labeled microtubules.[2, 34] At first, we introduced compound **1** to the motility assay system to assess its inhibitory activity toward kinesin. Figure 4(a) displays the dependence of the velocity of microtubule gliding on the concentration of compound **1**. A sharp decrease in the gliding velocity occurred upon increasing the concentration of **1** from 0 to 1.0 mM, reaching saturation near 1.5 mM, where the gliding velocity was 28 % of that under inhibitor-free conditions. This saturated inhibitor concentration of compound **1** is significantly higher than those in previous reports,[20, 34] possibly due to the different His tag position on the kinesin or to the buffer used in our experiments. Almost all of the microtubules maintained the same velocity even after the exposure of the sample to UV light, suggesting no influence of UV irradiation on the motility system containing compound **1**. Next, we introduced compound **4** to the motility assay system to assess its photoresponsive inhibition behavior. Unexpectedly, the inhibitory activity of the *trans* isomer of **4** was much higher than that of compound **1**. When we added the *trans* isomer of compound **4** at a concentration of 1.0 mM, the gliding velocity of the microtubules decreased to 4% of that observed under inhibitor-free conditions. Interestingly, upon irradiation of the sample with UV light, the

gliding velocity increased to 28% of that observed under inhibitor-free conditions. Upon irradiation with visible light, the gliding velocity decreased again. We could repeat this photoswitching of the gliding velocity for several cycles [See Figure 6(a) in section 3.4]. These findings reveal that the inhibitory activity of compound **4** changed reversibly along with its photoisomerization. Figure 4(b) displays the dependence of the gliding velocities of both the *trans* and *cis*-rich PSSs on the concentration of **4**. In the *trans* state, the gliding velocity decreased upon increasing the concentration of **4** from 0 to 1.0 mM, reaching saturation thereafter; in the *cis*-rich state, however, the gliding velocity decreased upon increasing the concentration of **4** up to 2.0 mM, but maintained relatively higher values. From these experiments, we conclude that the inhibitory effect of compound **4**—containing a peptide with an amino acid sequence derived from the kinesin's C-terminus tail domain and a terminal azobenzene unit—is greater than that of compound **1**, and that it also exhibits moderate phototunability of the inhibition effect at concentrations in the region 0.5–1.5 mM upon irradiation with UV or visible light.

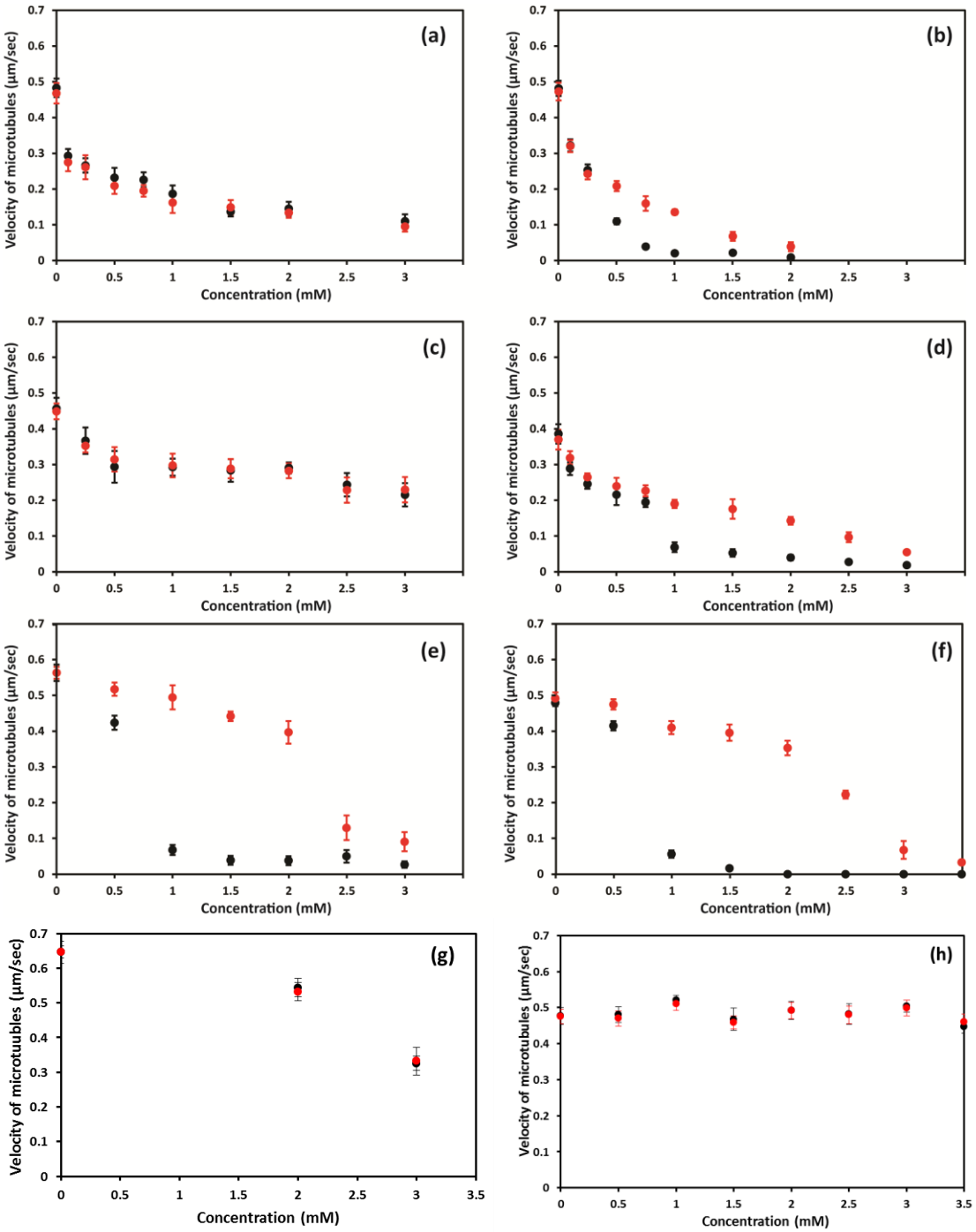

Figure 4. Gliding velocities of microtubules plotted with respect to the concentration of the inhibitory compounds; (a) compound **1**, (b) compound **4**, (c) compound **2**, (d) compound **5**, (e) compound **6**, (f) compound **8,** (g) compound **3**, (h) compound **7**. Black circles: gliding velocity in non-irradiated state; Red circles: gliding velocity after 365 nm light irradiation; Error bars represents the standard deviation for 10 microtubules.

3.3 Structural effect of azobenzene-peptides on the photo-switching properties

To enhance the phototunability further, we studied the role of the terminal functionality and the amino acid sequence of the peptides on the inhibition behavior. We synthesized two more compounds, **2** and **5** (Scheme 1 in section 3.1), with slight modification of the terminal functionality: the COOH groups of compounds **1** and **4** were replaced with $CONH_2$ groups, respectively. Figure 4(c) (section 3.2) displays the dependence of the velocity of microtubule gliding on the concentration of compound **2**. A decrease in the gliding velocity occurred upon increasing the concentration of **2** from 0 to 0.5 mM; thereafter, it reached a stable state in which its velocity remained constant up to 2.0 mM. At a concentration of approximately 2.5 mM, the gliding velocity suddenly decreased again. Figure 4(c) (section 3.2) also reveals that the inhibition effect of compound **2** was unaffected by UV light irradiation, similar to the behavior of compound **1**. Figure 4(d) (section 3.2) presents the dependence of the gliding velocity on the concentration of compound **5** in its *trans* and *cis*-rich PSSs. In the *trans* state, the gliding velocity decreased gradually upon increasing the concentration from 0 to 0.75 mM; at a concentration of approximately 1.0 mM, it suddenly decreased to a lower value, thereafter maintaining a saturated state up to 3.0 mM. In contrast, the *cis*-rich state revealed an initial decrease in velocity and almost saturation upon increasing the concentration to 1.5 mM, with a decrease in velocity again upon increasing the concentration of **5** from

1.5 to 3.0 mM. The second decrease in the gliding velocity of the *cis*-rich state at a concentration of **5** of approximately 2.5 mM is comparable to that obtained for compound **2**.

During many trials of synthetic azobenzene-peptides with the expectation of obtaining improved phototunability, we accidentally met with compound **6** (Scheme 1) (section 3.1) , which is the same as compound **5** in terms of the types and number of amino acid residues, with the only difference being the peptide sequence, which is the opposite of that in **5**. Figure 4(e) (section 3.2) displays the dependence of the gliding velocity on the concentration of **6** in both the *trans* and *cis*-rich PSSs. In the *trans* state, the gliding velocity decreased suddenly upon increasing the concentration of **6** above 0.5 mM, whereas the gliding velocity was maintained at a relatively high value at concentrations of up to 2.0 mM in the *cis*-rich state. We observed a drastic difference in velocity between the *trans* and *cis*-rich states of compound **6** at concentrations in the range between 1.0 and 2.0 mM. When we added the *trans* isomer of compound **6**, at a concentration of 2.0 mM, the gliding velocity of microtubules decreased to 12 % of that observed under the inhibitor-free conditions. Upon irradiation of the sample with UV light, the gliding velocity increased enormously, reaching a value almost identical to that under inhibitor-free conditions. Upon irradiation with visible light, the gliding velocity decreased again. We could repeat this photoswitching of the gliding velocity over many cycles [Figure 6(b)] (section

3.4). These findings suggest that the inhibitory activity of **6** changed reversibly along with its photoisomerization, with much higher efficiencies relative to those of compounds **4** and **5**. We observed a similar phenomenon even when we decreased the concentration of ATP from 1.0 to 0.1 mM [Figure 8(a)] (section 3.4), with abrupt decreases in velocity occurring at concentrations of compound **6** of 1.0 and 2.0 mM in its *trans* and the *cis*-rich states, respectively [Figure 5(a)]. The independence of the inhibitory activity of compound **6** on the ATP concentration supports a non-competitive inhibition mechanism[39] for both *trans* and the *cis*-rich states. Although compound **6** exhibited sufficient photoswitching ability of the gliding velocity upon alternating irradiation with UV and visible light, unfortunately the gliding velocity never reached zero (i.e., a stop or OFF state), even when we increased the concentration of **6** to greater than 3.5 mM in both the *trans* and *cis*-rich states.

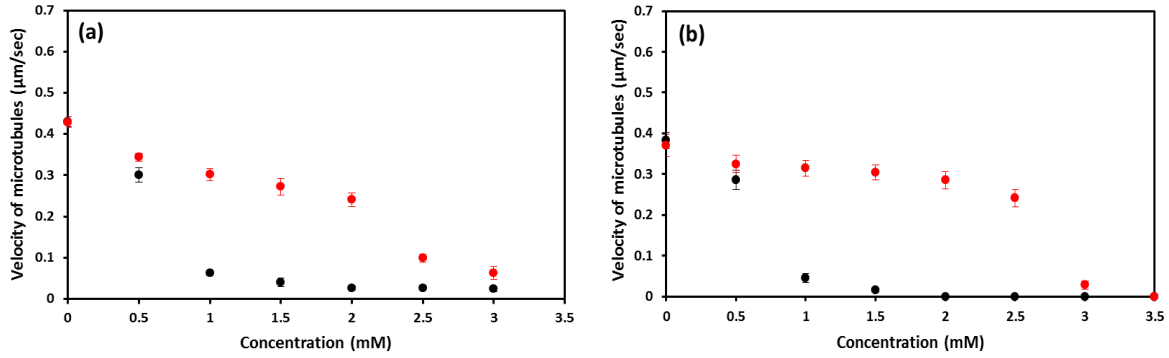

Figure 5. Gliding velocities of microtubules plotted with respect to the concentration of (a) compound **6**, (b) compound **8** at 0.1 mM ATP concentration. Black circles: gliding velocity of microtubules in non-irradiated state; Red

circles: gliding velocity after 365 nm light irradiation for 40 s; Error bars represents the standard deviation for 10 microtubules

3.4 Complete ON/OFF photoswitching and *in situ* control of the motility by an azobenzene-peptide

In a quest to identify the amino acid sequence in compound **6** that was most responsible for the photoresponsive inhibition properties, we synthesized and characterized three azobenzene-peptides—**7**, **8** and **9** (Scheme 1) (section 3.1)—each having part of the amino acid sequence of compound **6**. Despite having good solubility, compound **7**, which features the nine-amino-acid sequence of compound **6** from its arginine at the center to its N-terminus amino acid, exhibited no inhibition or photo effect, even at high concentrations. Indeed, we observed a stable velocity for the microtubules, regardless of the concentration of **7**, with no photo effect [Figure 4(h)] (section 3.2). In contrast, compound **8**, an 11-amino-acid sequence of compound **6** from the C-terminus arginine residue, displayed strong inhibitory activity, with the motion of almost all of the microtubules completely stopping when we added it at a concentration of 2.0 mM. Upon irradiation with UV light, all of the stopped microtubules began to move, with the gliding velocity increasing up to 0.4 μm/s. This finding indicates that a substantial ON/OFF control of the microtubule gliding occurred between the *trans* and *cis*-rich states. Upon irradiation with visible light, the moving microtubules stopped once again. We could repeat this photoswitching

between the “moving” and “stopping” states of the kinesin/microtubules for at least several cycles [Figure 6(c)]. We recorded a video of over five such cycles to further demonstrate the rapid and multiple regulations of this “moving” and “stopping” event *in situ* (Figure 7). We had difficulty in applying compound **9**, a five-amino-acid sequence of compound **6** from its C-terminus arginine residue, in the motility assay because of its low solubility in the buffer solution; therefore, we could not evaluate its inhibition properties or its changes upon irradiation. These results reveal the dependence of the gliding motion of the microtubules on the sequences of the reverse-ordered peptides. Among the three tested derivatives of compound **6** (compounds **7**–**9**), the reverse-ordered sequence in compound **8** exhibited perfect properties for controlling the switching of the gliding motion of microtubules at any desired point in time.

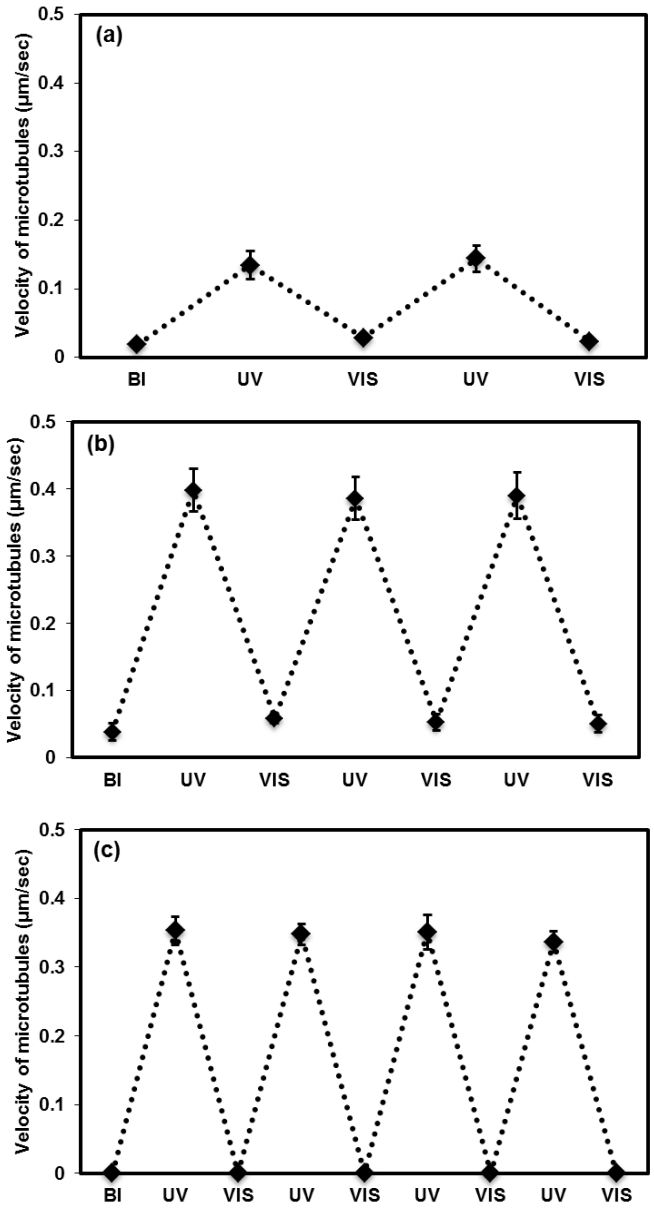

Figure 6. Repeatability of the Photo-controllable change in the gliding velocity of microtubules in presence of (a) compound **4** (1.0 mM), (b) compound **6** (2.0 mM), (c) compound **8** (2.0 mM) at 1.0 mM ATP concentration upon alternating irradiation with UV and visible light (BI: Before irradiation, UV: after 365 nm light irradiation for 40 s, VIS: after 436 nm light irradiation for 40 s). Error bars represents the standard deviation for 10 microtubules.

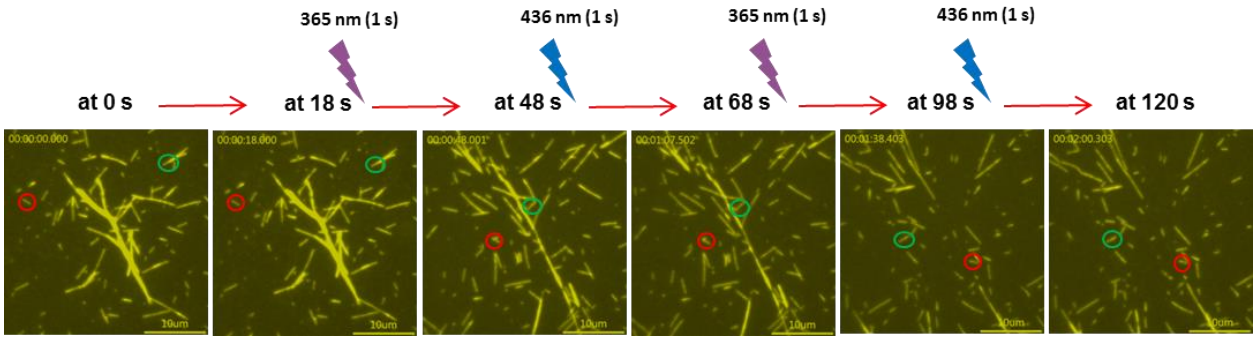

Figure 7. Fluorescence images of the gliding motility of microtubules on a kinesin-adsorbed glass surface in the presence of ATP (1.0 mM) and compound **8** (2.0 mM) during *in situ* photo controlling. Stop and move motions of microtubules were recorded after alternative irradiation with 436 nm (1 s) and 365 nm (1 s) lights respectively. Red and green circles indicate the positions of the selected microtubules.

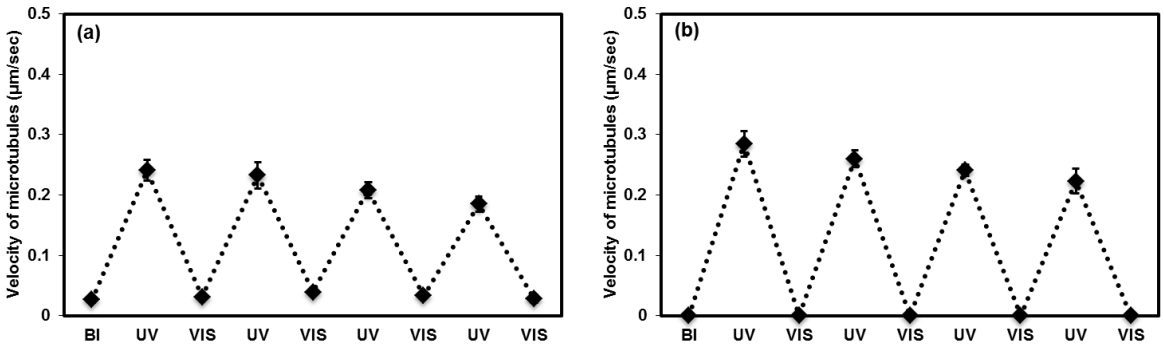

Figure 8. Repeatability of the Photo-controllable change in the gliding velocity of microtubules in presence of (a) compound **6** (2.0 mM), (b) compound **8** (2.0 mM) at 0.1 mM ATP concentration upon alternating irradiation with UV and visible light (BI: Before irradiation, UV: after 365 nm light irradiation for 40 s, VIS: after 436 nm light irradiation for 40 s). Error bars represents the standard deviation for 10 microtubules.

To explore the mechanism behind the photoresponsive inhibition properties of the azobenzene-peptides toward the activity of kinesin, we determined the rates of ATP hydrolysis in presence of the *trans* and *cis*-rich states of compound **8** using a malachite green colorimetric method, as explained in the Experimental section. Both the *trans* and *cis*-rich states of compound **8** inhibited the rate of ATP hydrolysis upon increasing their concentrations (Figure 9). At a concentration of **8** of approximately 1.5 mM, however, we observed a phenomenal variation—a change of 46%—in the rate of hydrolysis between the *trans* and *cis*-rich states. This finding suggests a clear influence of the azobenzene unit's isomerization on the rate of ATP hydrolysis. Nevertheless, the difference in the rates of hydrolysis obtained between the *trans* and *cis*-rich states of compound **8** at a concentration of approximately 1.5 mM did not correlate exactly with the difference obtained in the gliding velocity of the microtubules at the same concentration in the motility assay. This discrepancy might be due to different experimental conditions, including different concentrations of kinesin and microtubules. From these results, however, we conclude that the azobenzene-peptide **8** work as inhibitor for ATP hydrolysis and *trans* to *cis* isomerization switch the efficiency of the hydrolysis rate of ATP.

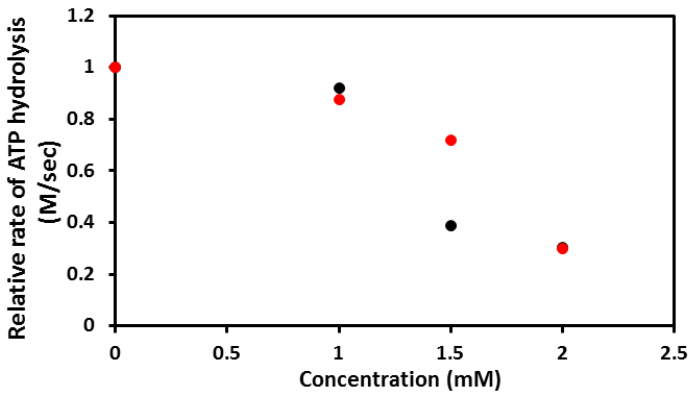

Figure 9. Rate of hydrolysis of ATP (1.0 mM) by kinesin/microtubules at various concentrations of compound **8** in its *trans* and *cis*-rich states. Black and red dots represent the reaction rates in presence of compound **8** in its *trans* and *cis*-rich states, respectively.

3.5 Spatiotemporal control over the gliding velocity of microtubules by an azobenzene-peptide

To demonstrate the spatiotemporal control over the gliding velocity of microtubules, we used the most efficient azobenzene-peptide **8**. We selectively irradiated an area of the flow cell of diameter 28 μm with 436 nm light and the whole area with 365 nm light at the same time [Figure 20, section 2.8]. The intensity of both the lights was well tuned to attain enough amount of *trans* **8** at the selected area where 436 nm was irradiated to completely stop the motion of microtubules. Once the actively moving microtubules under only 365 nm light reached to 436 nm light irradiating area, their motion was immediately stopped. As a result of this, density of the microtubules gradually increased at the

periphery (Figure 10c). When we removed the irradiation of 436 nm light, all the concentrated microtubules again started their motion under 365 nm light and got dispersed (Figure 10d). This local regulation of concentrating and dispersing of the microtubules was repeated for at least two cycles.

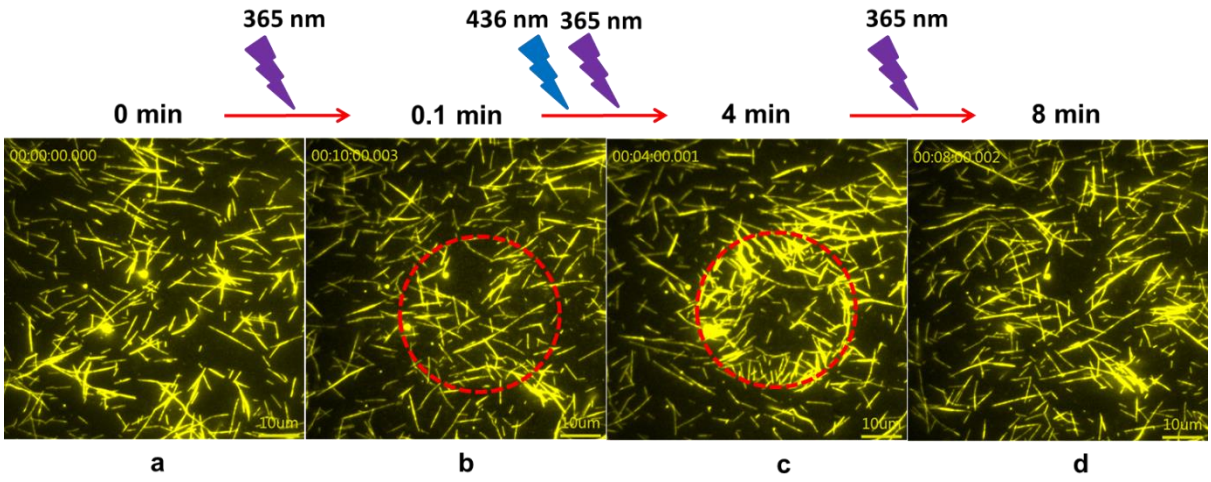

Figure 10. Fluorescence images of the gliding motility of microtubules on a kinesin-adsorbed glass surface in the presence of ATP (1.0 mM) and compound **8** (2.0 mM) during irradiation at the selected area using the setup shown in Figure 20 (section 2.8). The area inside the red circle was irradiated with 436 nm light and the whole area was irradiated with 365 nm light. (a) Before irradiation, (b) obtained after 365 nm light irradiation from 0 to 0.1 min, (c) obtained from (b) after 365 nm and 436 nm light irradiation at the same time from 0.1 to 4 min, (d) obtained from (c) after 365 nm light irradiation from 4 to 8 min.

3.6 Explanation of unconventional inhibition effect

Our results suggest that several structural features of the peptide inhibitor—namely, the presence and the stereochemistry of the azobenzene unit, the nature of the C-terminus, and the amino acid sequence—are tightly related to the inhibition efficiency.

The introduction of an azobenzene unit to the peptide from the C-terminus of kinesin increased the inhibition effect at concentrations in the region of over 250 μM [Figure 4(b)] (Section 3.2). Although we observed this effect for both of *trans*- and *cis*-azobenzene-peptides, the *trans*-azobenzene-peptides had the greater effect. Because serious inhibition of the peptides in the absence of the azobenzene unit occurred at concentrations in the region of less than 100 μM [Figure 4(a)] (Section 3.2), the effect of the azobenzene unit was to increase the maximum inhibition activity and to decrease the binding affinity to the motor system. In the case of compound **4**, featuring a C-terminal $CONH_2$ group, it is not clear whether the azobenzene-peptide interacted in the same mode as that of the compound **1**. In contrast, compound **5**, featuring a C-terminal COOH group, revealed at least two modes of inhibition with different affinities and inhibition efficiencies. The first inhibition mode operated at concentrations of less than 500 μM for both *trans*- and *cis*-**5** with similar efficiencies; the second, however, operated at different ranges of concentrations for the two regioisomers—namely, at approximately 800 μM for the *trans* isomer and approximately 2.2 mM for

the *cis* isomer [Figure 4(d)] (Section 3.2). We suspect that this difference in affinity to the binding site to induce inhibition was a result of a difference in either the hydrophobicity or shape of the isomers. This phenomenon is quite important in the quest for a large photoswitching effect because the difference in the concentration regions for the sharp drops in velocity induced by the *trans* and *cis*-azobenzene-peptides can result in a larger change in velocity upon photoisomerization being in the intermediate concentration range.

The reversal of the amino acid sequence diminished the initial inhibition effect observed in the sub-hundred micromolar region, while it enhanced the second one, observed at approximately 800 μM for the *trans*-azobenzene-peptide and at approximately 2.2 mM for the *cis*-azobenzene-peptide [Figure 4(e) and 4(f)] (Section 3.2). The change in velocity of the microtubules at concentrations in the range 1.0–2.0 mM upon photoisomerization became quite large with these two effects. From our study of compounds **7**, **8** and **9**, we found that the first 11 amino acid residues from the C-terminus of **6** were important for the inhibition effect, and for the change in the inhibition effect upon photoisomerization. It is known that the "IAK domain" in the tail region of kinesin is a highly conserved sequence, with mutation or deletion of this domain impairing inhibition of ATPase activity.[33, 34, 40] The large difference in the inhibition effects of **8**, which contains the KAI domain (namely, a "reverse IAK domain"), and **7**, which lacks the corresponding domain, indicates that this

sequence of three amino acids remains necessary for the inhibition effect, even in the reverse order. Maintaining the inhibition effect in regions of high concentration with the "reverse IAK domain" and impairing the primary inhibition effect at concentrations in the sub-hundred micromolar region with the reverse amino acid sequence were key features for obtaining such a large variation in the inhibition effect upon photoirradiation. Further experiments will be necessary to determine the exact molecular mechanism behind the complete stopping of the motility of the kinesin-microtubule system in the presence of compound **8**.

4. CONCLUSION

I have studied a new system to reversibly regulate the motility of kinesin-microtubules under external light stimuli in the presence of photoresponsive azobenzene-peptide inhibitors. I demonstrate herein complete photoregulation of the "ON" and "OFF" motions upon alternating irradiation with UV and visible light. To the best of our knowledge, this is the first to demonstration of a photoswitchable inhibitor that can reversibly regulate microtubule motility over many cycles. The advantage of employing photoresponsive unit to the inhibitors to regulate the gliding velocity of microtubules is that the velocity can be completely decreased to zero at sufficiently high concentrations of inhibitor, even in the presence of the less-effective isomer in the PSS. Such a motile property, exhibiting the complete zero velocity in the "OFF state" and the repeated switchability to be able to obtain the complete zero velocity again after attaining the "ON state" with reasonably high velocity, is in general necessary in artificial applications of motor proteins to nano transportation devices. Specifically, it would enable us to make an active spot with photo-generated *cis*-azobenzene-peptide allowing cargo-attached microtubules to move by irradiating with UV light selectively at any desired region. Such an active spot could be moved freely just by moving the position of UV light in an inactivated background irradiated with visible light keeping azobenzene-peptide in *trans*-rich state. In such a manner with a focused UV light we would select one specific microtubule attached with cargos and guide it to a desired point. As a

consequence, all kinds of transportation of nano-objects for separation, mixing, concentration would be possible. I expect that the complete photoregulation ability exhibited by compound **8** on the motility of kinesin-microtubules will aid in the development of real molecular machines working at will and open up new opportunities to design nano-transportation systems.[7–12]

5. REFERENCES

(1) Brady, S. T. A novel brain ATPase with properties expected for the fast axonal transport motor. *Nature* **1985**, 317, 73-75.

(2) Vale, R. D.; Reese, T. S.; Sheetz, M. P. Identification of a Novel Force-Genearating Protein, Kinesin, Involved in Microtubule-Based Motility. *Cell* **1985**, 42, 39-50.

(3) Howard, J. Mechanics of Motor Proteins and the cytoskeleton; Sinauer Press: Sunderland, MA, 2001.

(4) Hirokawa, N.; Noda, Y.; Okada, Y. Kinesin and dynein superfamily proteins in organelle transport and cell division. *Curr. Opin. Cell Biol*. **1998**, 10, 60-73.

(5) Vale, R. D. The Molecular Motor Toolbox for Intracellular Transport. *Cell* **2003**, 112, 467-480.

(6) Hirokawa, N.; Takemura, R. Molecular motors and mechanisms of directional transport in neurons. *Nat. Rev. Neurosci*. **2005**, 6, 201-214.

(7) Hiratsuka, Y.; Tada, T.; Oiwa, K.; Kanayama, T.; Uyeda, T. Q. P. Controlling the direction of kinesin-driven microtubule movements along microlithographic tracks. *Biophys. J*. **2001**, 81, 1555-1561.

(8) Van den Heuvel, M. G. L.; Dekker, C. Motor proteins at work for nanotechnology. *Science* **2007**, 317, 333–336.

(9) Bakewell, D. C. G.; Nicolau, D. V. Protein Linear Molecular Motor-Powered Nanodevices. *Aust. J. Chem*. **2007**, 60, 314-332.

(10) Agarwal, A.; Hess, H. Biomolecular motors at the intersection of nanotechnology and polymer science. *Prog. Polym. Sci*. **2010**, 35, 252-277.

(11) Aoyama, S.; Shimoike, M.; Hiratsuka, Y. Self-organized optical device driven by motor proteins. *Proc. Natl. Acad. Sci. U.S.A.* **2013**, 110, 16408-16413.

(12) Fujimoto, K.; Kitamura, M.; Yokokawa, M.; Kanno, I.; Kotera, H.; Yokokawa, R. Colocalization of Quantum Dots by Reactive Molecules Carried by Motor Proteins on Polarized Microtubule Arrays. *ACS Nano* **2013**, 7, 447–455.

(13) Hess, H.; Bachand, G. D.; Vogel, V. Powering nanodevices with biomolecular motors. *Chem. Euro. J*. **2004**, 10, 2110-2116.

(14) Hess, H. Self-assembly driven by molecular motors. *Soft Matter* **2006**, 2, 669-677.

(15) Hess, H.; Clemmens, J.; Qin, D.; Howard, J.; Vogel, V. Light-Controlled Molecular Shuttles Made from Motor Proteins Carrying Cargo on Engineered Surfaces. *Nano Lett*. **2001**, 1, 235–239.

(16) Bachand, G. D.; Rivera, S. B.; Boal, A. K.; Gaudioso, J.; Liu, J.; Bunker, B. C. Assembly and Transport of Nanocrystal CdSe Quantum Dot Nanocomposites Using Microtubules and Kinesin Motor Proteins. *Nano Lett*. **2004**, 4, 817-821.

(17) Diez, S.; Reuther, C.; Dinu, C.; Seidel, R.; Mertig, M.; Pompe, W.; Howard, J. Stretching and Transporting DNA Molecules Using Motor Proteins. *Nano Lett*. **2003**, 3, 1251-1254.

(18) Dinu, C. Z.; Opitz, J.; Pompe, W.; Howard, J.; Mertig, M.; Diez, S. Parallel manipulation of bifunctional DNA molecules on structured surfaces using kinesin-driven microtubules. *Small* **2006**, 2, 1090-1098.

(19) Higuchi, H.; Muto, E.; Inoue, Y.; Yanagida, T. Kinetics of force generation by single kinesin molecules activated by laser photolysis of caged ATP. *Proc. Natl. Acad. Sci. U.S.A.* **1997**, 94, 4395–4400.

(20) Nomura, A.; Uyeda, T. Q. P.; Yumoto N.; Tatsu, Y. Photo-control of kinesin-microtubule motility using caged peptides derived from the kinesin C-terminus domain. *Chem. Commun*. **2006**, 3588-3590.

(21) Martin, B. D.; Velea, L. M.; Soto, C. M.; Whitaker, C. M.; Gaber, B. P.; Ratna, B. Reversible control of kinesin activity and microtubule gliding speeds by switching the doping states of a conducting polymer support. *Nanotechnology* **2007**, 18, 055103-055109.

(22) Ionov, L.; Stamm, M.; Diez, S. Reversible switching of microtubule motility using thermoresponsive polymer surfaces. *Nano Lett*. **2006**, 6, 1982-1987.

(23) Volgraf, M.; Gorostiza, P.; Szobota, S.; Helix, M. R.; Isacoff, E. Y.; Trauner, D. Reversibly caged glutamate: a photochromic agonist of ionotropic glutamate receptors. *J. Am. Chem. Soc*. **2007**, 129, 260-261.

(24) Seki, T.; Nagano, S. Light-directed Dynamic Structure Formation and Alignment in Photoresponsive Thin Films. *Chem. Lett*. **2008**, 37, 484-489.

(25) Velema, W.A.; Van der Berg, J. P.; Hansen, M. J.; Szymanski, W.; Driessen, A. J. M.; Feringa, B.L. Optical control of antibacterial activity. *Nature Chem.* **2013**, 5, 924-928.

(26) Levitz, J.; Pantoja, C.; Gaub, B.; Janovjak, H.; Reiner, A.; Hoagland, A.; Schoppik, D.; Kane, B.; Stawski, P.; Schier, A.F et al. Optical control of metabotropic glutamate receptors. *Nature neuroscience* **2013**, 16, 507-518.

(27) Kuwahara, Y.; Kaji, M.; Okada, J.; Kim, S.; Ogata, T.; Kurihara, S. Self-alignment and photomechanical properties of alternative multi-layered films containing azobenzene polymer liquid crystal and polyvinyl alcohol layers. *Materials Letters* **2013**, 113, 202.

(28) Rahim, M. K. A.; Fukaminato, T.; Kamei, T.; Tamaoki, N. Dynamic photocontrol of the gliding motility of a microtubule driven by kinesin on a photoisomerizable monolayer surface. *Langmuir* **2011**, 27, 10347-10350.

(29) Kamei, T.; Fukaminato, T.; Tamaoki, N. A photochromic ATP analogue driving a motor protein with reversible light-controlled motility: controlling velocity and binding manner of a kinesin-microtubule system in an in vitro motility assay. *Chem. Commun*. **2012**, 48, 7625-7627.

(30) Perur, N.; Yahara, M.; Kamei, T.; Tamaoki, N. A non-nucleoside triphosphate for powering kinesin-microtubule motility with photo-tunable velocity. *Chem. Commun*. **2013**, 49, 9935-9937.

(31) Coy, D. L.; Hancock, W. O.; Wagenbach, M.; Howard, J. Kinesin's tail domain is an inhibitory regulator of the motor domain. *Nat. Cell Biol*. **1999**, 1, 288-292.

(32) Stock, M. F.; Guerrero, J.; Cobb, B.; Eggers, C.T.; T.-G. Huang, T. -G.; Li, X.; Hackney, D. D. Formation of the Compact Confomer of Kinesin Requires a COOH-terminal Heavy Chain Domain and Inhibits Microtubule-stimulated ATPase Activity. *J. Biol. Chem*. **1999**, 274, 14617-14623.

(33) Hackney, D.D.; Stock, M. F. Kinesin's IAK tail domain inhibits initial microtubule-stimulated ADP release. *Nat. Cell Biol*. **2000**, 2, 257-260.

(34) Yonekura, H.; Nomura, A.; Ozawa, H.; Tatsu, Y.; Yumoto, N.; Uyeda, T. Q. P. Mechanism of tail-mediated inhibition of kinesin activities studied using synthetic peptides. *Biochem. Biophys. Res. Commun*. **2006**, 343, 420-427.

(35) Howard, J.; Hudspeth, A. J.; Vale, R. D. Movement of microtubules by single kinesin molecules. *Nature* **1989**, 342, 154–158.

(36) Merino, E.; Ribagorda, M. Control over molecular motion using the cis-trans photoisomerization of the azo group. *Beilstein J. Org. Chem*. **2012**, 8, 1071-1090.

(37) Beharry, A. A.; Woolley, G. A. Azobenzene photoswitches for biomolecules. *Chem. Soc. Rev*. **2011**, 40, 4422–4437.

(38) Szymański, W.; Beierle, J. M.; Kistemaker, H. A. V.; Velema, W. A.; Feringa, B. L. Reversible Photocontrol of Biological Systems by the Incorporation of Molecular Photoswitches. *Chem. Rev*. **2013**, 113, 6114-6178.

(39) Segel, I. H. Enzyme Kinetics: Behavior and analysis of rapid equilibrium and steady-state enzyme systems; Wiley: New York, 1975.

(40) Seiler, S.; Kirchner, J.; Horn, C.; Kallipolitou, A.; Woehlke, G.; Schliwa, M. Cargo binding and regulatory sites in the tail of fungal conventional kinesin. *Nat. Cell Biol*. **2000**, 2, 333-338.

LIST OF PUBLICATIONS

1. K. R. Sunil Kumar, Takashi Kamei, Tuyoshi Fukaminato and Nobuyuki Tamaoki "Complete ON/OFF Photoswitching of the Motility of a Nano Biomolecular Machine", *ACS Nano*, 2014, DOI:10.1021/nn5010342

ACKNOWLEDGEMENTS

This dissertation would not have been possible without the guidance and the help of several individuals who in one way or another contributed and extended their valuable assistance in the preparation and completion of this study. It is a pleasure to convey my gratitude to them all in my humble acknowledgment.

Firstly I owe my deepest gratitude to the God, for his help and blessings to complete this research work.

This dissertation is completed first and foremost because of the supports and ideas of my supervisor, Professor Nobuyuki Tamaoki. Without his supervision, advice and suggestions from the very early stage of this research, it would be an impossible task. I would like to express great pleasure to acknowledge with sincere appreciation and deep sense of gratitude to him for giving me extraordinary experiences throughout the research. Above all and the most needed, he provided me unflinching encouragement and support in various ways. He is full with passion of science and constant oasis of ideas which exceptionally inspire and enrich my research work a great learning experience as a student as well as one of the unforgettable memories in my life.

I gratefully acknowledge Assistant Professors, Dr. Tsuyoshi Fukaminato, Dr. Takashi Kamei and Dr. Yuna Kim for their warm encouragement and involvement through important suggestion and helpful discussions.

I would like to thank Prof. Nishimura, Dr. Takahiko Matsushita and Dr. Fayna Maria Garcia Martin for their guidance in peptide synthesis and providing the laboratory instruments for the analysis.

I want to sincerely thank Dr. Reji Thomas, Dr. Oleksi Gutov, Dr. Mohammad Mustafa T.N and Dr. Rika Ochi for their experimental co-operation and valuable discussions.

I am grateful to our group's secretaries Arisa Hirade and Mariko Ooki who kept me organized and her indispensable help dealing with scholarship and administration during my research so I could optimally carry out my research and travels with poor Japanese language ability.

In my daily work I have been blessed with a friendly and cheerful group of fellow colleagues. I would sincerely appreciate and thankful all the members, Dr. Abdul Rahim M. K, Dr. Hashim P. K, Dr. Nishad Perur, Mr. Rijeesh K Nair, Ms. Halley M Menezes, Mr. Akasaka T, Mr. Yukinari K, Mr. Yahara M, Mr. Nakamoto Y, Mr. Ito S, Mr. Yoshida K, Ms. Amrutha A. S, Mr. Islam Md. Jahirul, Mr. Furuta R and the technical assistant Miss. Tateyama E, for their

kind experimental supports and sacrificial help. I am grateful to thank them deeply.

I would like to pay tribute to Hokkaido University, Japan to give me the opportunity to study in Japan and learn the culture and daily life of Japanese. I also want to express my sincere gratitude to Dr. Veena Prasad, Dr. C.V. Yelamaggad, Dr. Satish Patil (my honorable supervisors during my work as a research assistant) for their guidance and advice throughout my career.

I gratefully acknowledge the program organizers of IGP-RPLS that made my Ph.D a reality.

My family deserves special mention for their inseparable support and prayers. I would like to thank all my family members including my parents, brothers, sisters, uncles, aunts and also my beloved friends for their psychological support and encouragement during my career.

Last but not the least; I would like to thank everybody who was important to the successful realization of thesis and my career as well as expressing my apology that I could not mention personally one by one.

Sunil Kumar K R